HHS Public Access

Author manuscript

Cell. Author manuscript; available in PMC 2018 April 20.

Published in final edited form as:

Cell. 2017 April 20; 169(3): 497–509.e13. doi:10.1016/j.cell.2017.03.044.

Spontaneous chitin accumulation in airways and age-related fibrotic lung disease

Steven J. Van Dyken[1], **Hong-Erh Liang**[1], **Ram P. Naikawadi**[1], **Prescott G. Woodruff**[1], **Paul J. Wolters**[1], **David J. Erle**[1], and **Richard M. Locksley**[1,2,3,*]

[1]Departments of Medicine, University of California, San Francisco, San Francisco, California 94143, USA

[2]Microbiology & Immunology, University of California, San Francisco, San Francisco, California 94143, USA

[3]Howard Hughes Medical Institute, University of California, San Francisco, San Francisco, California 94143, USA

SUMMARY

The environmentally widespread polysaccharide chitin is degraded and recycled by ubiquitous bacterial and fungal chitinases. Although vertebrates express active chitinases from evolutionarily conserved loci, their role in mammalian physiology is unclear. We show that distinct lung epithelial cells secrete acidic mammalian chitinase (AMCase), which is required for airway chitinase activity. AMCase-deficient mice exhibit premature morbidity and mortality, concomitant with accumulation of environmentally-derived chitin polymers in the airways and expression of pro-fibrotic cytokines. Over time, these mice develop spontaneous pulmonary fibrosis, which is ameliorated by restoration of lung chitinase activity by genetic or therapeutic approaches. AMCase-deficient epithelial cells express fibrosis-associated gene sets linked with cell stress pathways. Mice with lung fibrosis due to telomere dysfunction and humans with interstitial lung disease also accumulate excess chitin polymers in their airways. These data suggest that altered chitin clearance could exacerbate fibrogenic pathways in the setting of lung diseases characterized by epithelial cell dysfunction.

Graphical abstract

eTOC: An ancient enzyme protects the lungs from damaging effect of a widespread environmental allergen.

*Corresponding Author /Lead Contact: Dr. Richard M. Locksley, University of California, San Francisco, 513 Parnassus Ave, S-1032B, San Francisco, CA 94143-0795, Telephone: 415-476-5859; FAX: 415-502-5081, richard.locksley@ucsf.edu.

AUTHOR CONTRIBUTIONS

S.J.V.D. performed experiments, analyzed data and wrote the manuscript. S. J.V.D. and H-E.L. generated ChiaRed mice. D.J.E. provided expertise with RNA-Seq experiments. P.J.W. and P.G.W. provided BAL fluid samples from human subjects, and R.P.N. and P.J.W. provided unpublished data and BAL fluid from conditional TRF-1 deficient mice. R.M.L. directed the studies and wrote the manuscript with S.J.V.D.

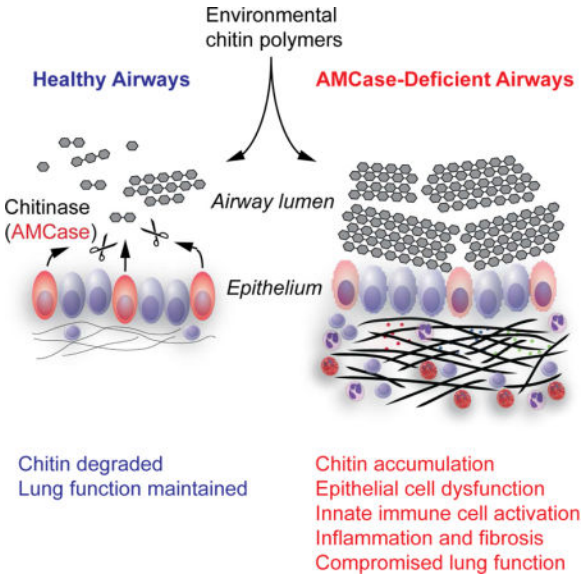

Keywords

AMCase; chitin; chitinase; epithelium; pulmonary fibrosis; interleukins; interstitial lung disease; age-related disease; polysaccharide

INTRODUCTION

Mucosal barrier dysfunction and immune activation are associated with age-related fibrotic lung diseases, but environmental stimuli that incite these pathways remain largely uncharacterized (Travis et al., 2013; Rockey et al., 2015). The abundant polysaccharide chitin, which is widely dispersed in both terrestrial and aquatic settings as a rigid, insoluble constituent of fungi, insects, helminths and arthropods, is a candidate environmental insult that initiates innate immune cell activation when aspirated into the lung (Reese et al., 2007; Van Dyken et al., 2011; 2014). Mammals express several family 18 glycosyl hydrolases, which in mice and humans include enzymatically inactive chi-lectins and two active chitinases, chitotriosidase (Chit1) and acidic mammalian chitinase (AMCase; *Chia1*), an evolutionarily conserved secreted enzyme that is constitutively expressed in the lung and stomach and also highly induced during STAT6-dependent immune responses (Reese et al., 2007; Hussain & Wilson, 2013). Elevated serum Chit1 is associated with Gaucher disease (Adrangi & Faramarzi, 2013) and, although AMCase was originally proposed to mediate reactive airways disease (Zhu et al., 2004), two separately generated AMCase transgenic mice exhibit normal lung function and do not develop lung disease (Reese et al., 2007; Fitz et al., 2012). Rather, these mice remain resistant to epithelial and lymphoid cell-mediated inflammatory injury in response to inhaled or aspirated chitin (Reese et al., 2007; Van Dyken et al., 2011; 2014). Conversely, attenuation of chitinase or AMCase activity increases inflammatory cell accumulation and delays resolution after acute chitin challenge (Van Dyken et al., 2011; Fitz et al., 2012; Kim et al., 2015), consistent with an enzymatic role for AMCase in the degradation of insoluble chitin polymers and suggesting that increased

chitinolytic activity represents a conserved feedback mechanism to limit mucosal inflammatory responses in mammals.

Chitinases and chi-lectins are widely conserved throughout phylogeny, sharing similar protein domain architecture; in mammals, active chitinases are often present in multiple copies, arising from an initial duplication event of the ancestral enzyme that coincided with expansion of the vertebrate chitinase family (Hussain & Wilson, 2013). In both mice and humans, genes encoding active chitinases AMCase and Chit1 are flanked by enzymatically inactive chi-lectins, several of which have been linked to inflammatory and fibrotic diseases by mechanisms that remain unclear; notably, a common 24-bp duplication in human *CHIT1* results in the expression of an inactive enzyme with little evident phenotypic consequence, even in populations exposed to chitin-rich foods and enteroparasites (Hussain & Wilson, 2013; Adrangi & Faramarzi, 2013; Manno et al., 2014; Sutherland et al., 2014; Zhou et al., 2014). Considerable complexity underlies polysaccharide degradation in prokaryotes and eukaryotes, which can be coordinated by multimeric protein assemblies consisting of active enzymes and lectin-like binding proteins that support wide-ranging processes including morphogenesis, nutrient acquisition, and innate immunity (Adrangi & Faramarzi, 2013; Smith & Bayer, 2013; Schwartzman et al., 2015). Whether AMCase and/or Chit1 coordinate similar chitinolytic activities in the context of normal mammalian physiology, however, has remained unclear due to discrepancies in biochemical activity assays, conflicting reports, and lack of specific reagents and systems to track and characterize relevant cells and molecules.

Given the widespread distribution of chitin substrates in the environment, we sought to determine whether mammalian chitinases such as AMCase and Chit1 function to mediate degradation and facilitate clearance of this ubiquitous insoluble polysaccharide at mucosal barriers under normal physiologic conditions. Here, using an AMCase knockin/knockout reporter mouse, we describe a population of lung epithelial cells that express AMCase necessary for chitin degradation in the airways, revealing a constitutive pathway important in clearing chitin oligomers and in preventing age-related fibrosis and decline in lung health. We present additional evidence that dysfunction of this homeostatic pathway may be relevant to other fibrotic lung diseases in mice and humans.

RESULTS

Airway endochitinase activity is mediated by AMCase-expressing epithelial cells

To investigate the source and physiologic role of AMCase, we generated tandem dimer red fluorescent protein (tdTomato)-Cre knockin/knockout mice, termed “ChiaRed” (Figure 1A, Figure S1A and S1B). Two targeted ChiaRed clones were bred and characterized; homozygous ChiaRed (C/C) mice were born at Mendelian ratios and exhibited no obvious developmental abnormalities. We analyzed lymphoid and nonlymphoid tissues (lung, stomach, peritoneal cavity, spleen, mesenteric lymph nodes) by flow cytometry and, although previous studies have suggested that AMCase is derived from macrophages (Zhu et al 2004; Kim et al., 2015), we observed no AMCase expression (as assessed by tdTomato) in CD45+ hematopoietic cells either at rest or after infection with *Nippostrongylus brasiliensis* (*Nb*), a migratory helminth that elicits a robust type 2 immune response associated with

AMCase induction (Figure S1C–E and data not shown; Reese et al., 2007). Among CD45- lung cells, however, we observed a population of AMCase-expressing cells that co-expressed the epithelial cell marker, EpCAM (Figure 1B). These cells localized to both conducting and distal airway epithelium and shared protein markers for secretory cells including type 2 alveolar epithelial cells (surfactant protein C), but were distinct from Foxj1-expressing ciliated cells (Figure 1C, Figure S2A and S2B). In confirmation of this lung expression pattern, *Chia1* mRNA was detected in sorted CD45-EpCAM+ lung epithelial cells but not in alveolar macrophages, which, in contrast, expressed high levels of *Chil3*, encoding the chi-lectin Ym1 (Figure 1D). RNA-Seq analysis of sort-purified ChiaRed reporterexpressing lung epithelial cells from heterozygous mice also indicated significant enrichment of secretory cell marker genes (e.g., *Scgb1a1, Scgb3a2, Cyp2f2, Muc5b*; Kotton & Morrisey, 2014) among ChiaRed+ epithelial cells as compared to unfractionated lung epithelial cells (CD45-EpCAM+) from wild-type mice; however, markers associated with distal alveolar cell types, such as *Sftpc* and *Sftpb*, were also highly expressed in both cell populations, albeit not differentially, indicating that AMCase is expressed by a subset of secretory lung epithelial cells including club cells and type 2 alveolar cells lining proximal and distal airways (Figure 1E and Table S1).

Lung AMCase mRNA was absent in homozygous ChiaRed mice, while expression of chi-lectins remained normal; notably, the other mammalian chitinase capable of mediating endochitinase activity, chitotriosidase (*Chit1*), was not detected in lung tissue from wild-type, AMCase transgenic (lung-specific; SPAM, Reese et al., 2007) or AMCase-deficient mice (Figure 1F). Consistent with this, AMCase, but not Chit1, protein was readily detected in bronchoalveolar lavage (BAL) fluid of wild-type mice but absent in homozygous ChiaRed mice (Figures 1G and Figure S2C). Chitinase (chitobiosidase and chitotriosidase) activity in the BAL fluid, both in steady-state and after *Nb* infection, was abolished in homozygous ChiaRed mice, while β-N-acetylglucosaminidase activity, which can be mediated by hexosaminidases, was unaffected (Figure 1G and Figure S2D). Thus, epithelial AMCase mediates lung endochitinase activity in the steady-state and after augmentation by type 2 cytokine signaling, consistent with prior findings in gene-targeted mice (Fitz et al., 2012).

Constitutive AMCase expression is independent of type 2 cytokine signaling

The type 2 cytokines IL-4 and IL-13, along with their shared signaling adapter STAT6, mediate AMCase induction in the lungs following type 2 immune challenges such as allergens and helminths (Zhu et al., 2004; Reese et al., 2007). We assessed whether the ChiaRed reporter allele was responsive to exogenous type 2 cytokine stimulation by administrating IL-13 into the airways of heterozygous ChiaRed mice. This treatment increased both the percentage of epithelial cells that expressed the ChiaRed reporter and the median fluorescence intensity (MFI) of tdTomato among reporter-expressing cells (Figure 2A–C); similar induction was also observed in ChiaRed reporter mice crossed to a lung-specific IL-13 transgene (data not shown). Airway chitinase activity in the steady-state, however, was not dependent on either STAT6 or IL-4/13, and endochitinase activity in BAL fluid was normal in mice with genetic deficiencies in either STAT6 or IL-4/13 (Figure 2D). Further, although ChiaRed reporter expression was highly induced in epithelial cells after *Nb* infection in a STAT6-and IL-4/13-dependent manner, consistent with prior lung

expression data (Reese et al., 2007), constitutive ChiaRed expression in these cells remained normal in the absence of type 2 cytokine signaling (Figure 2E and 2F). Thus, the ChiaRed reporter accurately reflects AMCase activity as based on prior reports.

Constitutive AMCase maintains lifespan and lung health with aging

Although young mice maintained in standard barrier conditions exhibited no overt signs of disease, we noted spontaneous progressive health decline in a significant proportion of aging AMCase-deficient mice housed in standard barrier conditions, variably characterized by hunched posture, labored breathing, poor grooming/hair loss, skin lesions, and death (Figure 3A; moribund mice were euthanized as recommended by veterinary staff). In 12-month-old AMCase-deficient mice, oxygen saturation levels were significantly lower than in similarly aged wild-type controls, consistent with impaired lung function (Figure 3B). Analysis of lung tissue from 6–9 month-old AMCase-deficient mice revealed a pleomorphic accumulation of inflammatory immune cells, including group 2 innate lymphoid cells (ILC2s), γδ T cells, CD4+ T cells, eosinophils, and neutrophils (Figure 3C), which resembled the profile of the lung cellular infiltrate induced after acute inhalation of purified chitin in wild-type mice (Van Dyken et al., 2014). Although resident lung CD4+ T cells were elevated in aged ChiaRed homozygotes, the TCR Vβ repertoire among these cells and serum IgE and IgG_1 antibody levels were unaffected by the absence of AMCase, suggesting that predominately innate immune pathways were dysregulated in the lungs of aging AMCase-deficient mice (Figure 3D–F).

AMCase-deficient mice develop spontaneous age-related lung fibrosis

Activation of resident lung ILC2s and γδ T cells after chitin inhalation induces IL-13 and IL-17A production from these cells, respectively (Van Dyken et al., 2014); both cytokines have been implicated in the pathogenesis of lung fibrosis (Wilson et al., 2010). We bred AMCase-deficient mice onto rFNγ/rL-17A/IL-5/IL-13 cytokine reporter backgrounds (Price et al., 2012; Nussbaum et al., 2013; Liang et al., 2011) to assess the spontaneous expression of these cytokines among resident lung lymphocyte populations. We observed significantly increased percentages of lymphoid cells expressing these cytokines among CD4+ T cells, γδ T cells, and ILC2s in the lungs of AMCase-deficient mice as compared to wild-type controls. Cytokine-expressing cells became more pronounced with age (Figure 4A–C), a finding consistent with the mixed neutrophil and eosinophil infiltrates, and suggested that persistent cytokine-mediated immune stimulation contributed to chronic tissue alterations. Indeed, AMCase-deficient mice spontaneously developed age-related lung fibrosis, evidenced by increased subepithelial collagen deposition that was most prominent around conducting airways and vasculature (Figure 4D), but also accompanied by alveolar septal thickening and infiltration (Figure S3A and S3B). Blinded histopathologic scoring of parenchymal changes using the Ashcroft scale (Hübner et al., 2008) revealed higher fibrosis scores among 9-month-old AMCase-deficient animals as compared to age-matched wild-type mice (Figure 4E), and correlated with significantly increased lung hydroxyproline levels (Figure 4F). Aged AMCase-deficient animals also exhibited dysregulated immune responses to helminth infection, consistent with systemic inflammation (Finkelman et al., 1994). Thus, intestinal clearance of *Nb* was delayed in older mice but unaffected in young AMCase-deficient mice as compared to littermate control wild-type mice, consistent with a

separate study that did not examine the effects of age (Figure S4A–C; Vannella et al., 2016a).

Chitin accumulates spontaneously in the airways of aged AMCase-deficient mice and contributes to fibrosis

Chitin biopolymers are substrates for active chitinases and structurally related chi-lectins (Hussain & Wilson, 2013; Schimpl et al., 2012). While Ym1 protein, a STAT6-inducible chi-lectin genetically positioned near *Chia1* and associated with lung inflammation (Sutherland et al., 2014) was present in BAL fluid, it was not altered in young or aged AMCase-deficient animals at rest or 10 days after infection with *Nb* (Figure 5A). Chitinase activity in the BAL fluid of AMCase-deficient animals, however, remained undetectable with age, revealing a non-redundant function for this enzyme (Figure 5B), and raising the possibility that altered chitin turnover in the airways contributed to age-related lung fibrosis. Indeed, BAL fluid isolated from AMCase-deficient mice at ages corresponding with fibrosis contained significantly elevated levels of spontaneously acquired chitin fragments than did wild-type controls, as assessed using a highly-specific chitin-binding-domain (CBD)-containing probe (Figure 5C; Watanabe et al., 1994). These chitin fragments likely derived from sources in the immediate environment of the mice. Consistent with this, we detected CBD-positive constituents sensitive to chitinase degradation in autoclaved plant-derived food and bedding materials used in the rodent barrier housing facility (Figure 5D), suggesting that in aged AMCase-deficient mice, the inability to degrade ubiquitous, complex environmental sources of chitin mediates persistent epithelial stimulation, immune activation, and fibrosis.

To further test the direct effects of environmentally-derived chitin, we administered extracts of house dust mite (*Dermatophagoides farinae*) and mold (*Aspergillus niger*), each of which contains chitin elements sensitive to chitinase degradation, to wild-type and AMCase-deficient mice (Figure S5A, B). At times when wild-type mice resolved inflammation, AMCase-deficient mice retained significant accumulations of gd T cells, CD4+ T cells, neutrophils and eosinophils (Figure S5C), supporting prior studies linking AMCase activity inversely with chitin levels and lung inflammation (Reese et al., 2007; Fitz et al., 2012; Van Dyken et al., 2011; 2014; Kim et al., 2015), and consistent with delayed resolution due to altered chitin clearance. Depletion of chitin from *A. niger* by pre-treatment with active chitinase reduced total BAL chitin levels in AMCase-deficient animals after challenge (Figure S5D), thus restoring the resolution of inflammation (Figure S5E), while challenge with purified chitin led to increased accumulation of γδ T cells and neutrophils in the lungs of AMCase-deficient mice (Figure S5F). We also observed significantly higher numbers of lung ILC2s, γδ T cells and IL-17A-producing γδ T cells in AMCase-deficient mice throughout the enhanced response to *A. niger* (Figure S5G, H), consistent with increased activation of lymphoid cell populations and production of pro-fibrotic cytokines by persistent chitin-mediated injury.

To address whether restoration of lung chitinase activity was able to impact disease in the context of spontaneously accumulated environmental chitin fragments, we generated mice with lung-specific (surfactant protein C promoter-driven) transgenic expression of AMCase on a ChiaRed homozygous background (SPAM x CC). BAL chitobiosidase activity was

robustly restored in SPAM x CC mice, to levels approximately 10-fold higher than in BAL collected from wild-type animals (Figure 5E). This restoration significantly reduced the levels of chitin polymers in the airways of 9-month-old SPAM x CC mice compared to co-housed littermate CC mice (Figure 5F). Remarkably, lung-specific transgenic AMCase restoration also ameliorated the inflammatory infiltrates and fibrosis in aged CC mice (Figure 5G and 5H), consistent with a role for AMCase in mediating homeostatic degradation and turnover of immunostimulatory environmental chitin. To additionally test whether restoration of chitinase enzymatic activity was sufficient to ameliorate disease, we instilled recombinant Chit1 into the airways of aged AMCase-deficient mice repeatedly for 3 weeks. This regimen significantly elevated airway chitobiosidase activity for 48 hours after each dose, although this level remained below that of wild-type mice (Figure 5I). In agreement with the genetic chitinase restoration, treatment with Chit1 significantly reduced chitin polymer accumulation in the BAL of aged AMCase-deficient mice (Figure 5J), along with percentages of cytokine-expressing lymphoid cells, particularly IL-17-expressing CD4+ T cells and γδ T cells, as well as IL-13-expressing ILC2s in the lungs of AMCase-deficient mice as compared to wild-type controls (Figure 5K). Furthermore, we observed a significant reduction in the hydroxyproline content of the lungs treated with Chit1 as compared to PBS (Figure 5E), suggesting that abnormal chitin accumulation contributed to pro-fibrotic cytokine production and the severity of fibrosis, which was responsive to enzyme replacement therapy in the context of AMCase deficiency and aging.

Cytokine signaling and cellular stress pathways induced in AMCase-deficient epithelium

Homeostatic maintenance of the airways requires anticipatory production of enzymes, scavengers, and other factors moderating cellular stress pathways in response to periodic environmental insults, including exposures to pollutants, toxins, particulates, and endogenously produced reactive metabolites (Wolters et al., 2014; Sundar et al., 2015). The abnormal accumulation of chitin particles and the development of fibrosis in aged AMCase-deficient mice suggested that disease was initiated by epithelial dysfunction. To identify molecular pathways altered in the absence of AMCase, we performed RNA-Seq to compare the transcriptomes of ChiaRed reporter-positive epithelial cells isolated from the lungs of 12-week-old heterozygous and homozygous mice, prior to the onset of lung fibrosis. Strikingly, 1463 genes that were expressed at a level of > 100 fragments per kilobase of exon per million mapped reads (FPKM) in either one of the cell populations were differentially expressed between C/+ and C/C epithelial cells [false discovery rate (FDR) < 0.05; Table S2], indicating broad transcriptomic changes in the absence of AMCase. Pathway analysis indicated significant alterations between AMCase-deficient homozygous and heterozygous ChiaRed+ epithelial cells in a wide array of canonical pathways, including those involved in maintaining cellular integrity and cytokine signaling (Figure 6A and Table S3), revealing the induction of these pathways prior to the onset of fibrotic disease in AMCase-deficient animals. Gene sets belonging to pathways including NRF2-mediated oxidative stress responses (e.g., *Nfe2l2, Fos, Actb, Maff*), unfolded protein responses (*Xbp1, Atf4*), NF-κB signaling (*Il33, Nfkbib*), telomerase signaling (*Hsp90aa1, Myc*), and circadian rhythms (*Per1, Per2, Cry1, Cry2*) were statistically overrepresented in AMCase-deficient cells as compared to heterozygous cells (Figure 6B). These results suggest that the inability to efficiently clear chitin particles from the airways initiates activation of epithelial cell stress

pathways, inflammatory immune signaling, and dysregulation of homeostatic barrier function, all processes previously implicated in the development of lung fibrosis (Wolters et al., 2014; Sundar et al., 2015).

The prominent cytokine signature that accompanied these early epithelial alterations led us to further test the persistent involvement of the type 2 cytokines IL-4, IL-5, and IL-13 in fibrotic disease associated with AMCase deficiency and aging. Chitin acutely induces IL-5 and IL-13 production from lung-resident ILC2 cells, which mediates eosinophilia in a manner partially dependent on the epithelial cytokine IL-33 (Van Dyken et al., 2014; Mohapatra et al., 2016), and *Il33* transcript was significantly elevated in AMCase-deficient cells from young mice (Figure 6B). Although IL-5 deficiency eliminated the lung eosinophil accumulation in aged CC animals, this reduction had no effect on the lung fibrosis as measured by hydroxyproline content (Figure S6A–C). In contrast, loss of IL-4 and IL-13 or their signaling adapter STAT6 profoundly exacerbated fibrotic lung disease and death rates in aging CC animals (Figure 6C and 6D), indicating that certain type 2 cytokine-mediated pathways protect against severe lung injury, enhanced fibrosis, and death in the context of AMCase deficiency, consistent with a recent report documenting similar worsening in response to bleomycin-mediated lung injury among IL-13Ra1-deficient mice (Karo-Atar et al., 2016).

Human ILD patients accumulate chitin polymers in BAL fluid

Age-related pulmonary fibrosis in humans can be associated with chronic exposure to insoluble particles, such as asbestos, silica and beryllium, and recently, activated ILC2s were implicated in the pathogenesis (Hams et al., 2014). We readily detected AMCase protein in BAL fluid from healthy human controls and patients with interstitial lung disease [ILD; comprising idiopathic pulmonary fibrosis (IPF) or pulmonary fibrosis associated with scleroderma; Table S4] or asthma; as in the mouse, the other human chitinase, chitotriosidase, was not prevalent (Figure 7A and Figure S7A). We observed no difference in AMCase protein levels in BAL fluid between controls and patients with ILD or asthma (Figure 7B and Figure S7B). AMCase activity can vary with common gene polymorphisms (Seibold et al., 2009; Aminuddin et al., 2012; Okawa et al., 2016), but no differences in exo- or endochitinase activity were observed in BAL fluid between controls and patients with ILD; however, notably, human endochitinase activity in all but one patient sample was comparatively lower than in mouse BAL fluid, and in contrast to normal β-N-acetylglucosaminidase activity (Figure 7C), supporting prior studies describing relatively inefficient enzymatic activity among common human AMCase isoforms (Seibold et al., 2009; Goedken et al., 2011; Okawa et al., 2016). Further, as assessed using CBD-reactive material, significantly increased amounts of chitin polymers were present in BAL fluid from patients with ILD as compared to healthy controls (Figure 7D). This accumulation of chitin polymers was significant in patients with either IPF or pulmonary fibrosis associated with scleroderma and did not appear to be a generalized feature of lung inflammatory disorders, since the low level of chitin in the BAL fluid from patients with asthma did not differ from healthy controls (Figure S7C and S7D). In further support of this, mice that develop pulmonary fibrosis due to the conditional deletion of the protective telomere factor TRF-1 in alveolar type II cells (Povedano et al., 2015; Naikawadi et al., 2016) also accumulated chitin

polymers in the airways with age (Figure 7E), indicating that induction of epithelial dysfunction alone was sufficient to impair chitin clearance from the airways. These data suggest that physiologic control of environmental chitin may not be maintained in the setting of abnormal fibrotic lung architecture and aging, perhaps reflecting impaired mucociliary clearance, cellular stress, or epithelial dysfunction in combination with low AMCase activity, or the inability to induce endochitinase production to high levels similar to those invoked by robust type 2 immunity and STAT6-mediated repair pathways (Figure 1G).

DISCUSSION

Here, we show that AMCase is a constitutively secreted and non-redundant enzyme that mediates the clearance of environmental chitin from healthy airways. In its absence, we observe significant morbidity and mortality in mice associated with accumulation of chitin polymers and persistent activation of immune cells and cytokines previously implicated in low-grade inflammation and fibrosis. Chitin is an insoluble biopolymer dispersed throughout the environment (Keyhani & Roseman, 1999), including urban home environments (Van Dyken et al., 2011); individuals commonly have antibodies to ubiquitous chitin-associated allergens from insects and molds, consistent with widespread chitin exposure (Salo et al., 2014). Reducing airway chitinase activity in mice alters the normal resolution of inflammation following challenge with complex biologic chitin-containing constituents, including house dust mite and fungal extracts (Van Dyken et al., 2011, Kim et al., 2015), implicating a contributory inflammatory role for chitin even in the presence of multiple other pattern recognition elements present in dust mite and fungal preparations. Our results suggest that chitin degradation by chitinase is a constitutive and essential process that maintains lung homeostasis, since aged AMCase-deficient mice develop spontaneous lung fibrosis in association with activated cytokine and molecular pathways previously implicated in this process (Wilson et al., 2010; Wolters et al., 2014). Therapeutic administration of exogeneous chitinase to the airways reduced fibrosis in aged animals, suggesting that restoring the ability to clear or degrade naturally-acquired chitin particles can ameliorate persistent stimulation of innate inflammatory pathways associated with chitin particle accumulation and lung disease.

Acute inhalation of purified chitin particles initiates the epithelial cytokine-driven activation of resident lymphoid cells that orchestrate parallel pathways of IL-17-and IL-13-mediated inflammation associated with a mixed neutrophil and eosinophil infiltrate (Van Dyken et al., 2014). Specialized AMCase-expressing lung epithelial cells, as revealed by the ChiaRed reporter mouse, are critical in mediating the degradation and clearance of the stimulus and thereby act as negative regulators of the persistent inflammatory pathways that mirror the pattern of cell and cytokine activation triggered by experimental acute chitin exposure in wild-type mice. Although the persistent lack of airway endochitinase activity in aged AMCase-deficient animals indicates that Chit1 does not compensate in this setting, replacement of chitinase activity by Chit1 administration to the airways of AMCase-deficient mice was sufficient to reduce chitin levels, ameliorate cytokine expression, and lessen fibrosis, highlighting the essential role for this specific enzymatic activity in the airways. Notably, similar patterns of inflammation to those induced by chitin occur in response to an array of lung epithelial tissue perturbations containing chitin, including

helminth infection, dust mite, protease and fungal exposures (Mohapatra et al., 2016; Van Dyken et al., 2016), and may contribute to lung fibrosis when dysregulated (Vannella et al., 2016b). These stereotyped cytokine networks in response to lung injury may connect general pathways of epithelial dysfunction (oxidative stress, activation of UPR, periodic cycling) with tissue inflammation that, in the case of AMCase deficiency, can be exacerbated by accumulation of particles normally cleared through enzymatic degradation or, in other pathologic settings, through impaired mucociliary function or anatomic disruption. A complex interplay between the epithelium and associated cytokines, however, was revealed by the exacerbation of the AMCase-deficiency phenotype in the absence of IL-4/IL-13 signaling, indicting that protective factors are simultaneously engaged in the context of immune stimulation.

Although AMCase expression in the steady-state is required to prevent spontaneous disease associated with accumulation of chitin polymers, low levels of AMCase expression or activity in the context of fibrosis or aging may be unable to mediate efficient chitin clearance or degradation, as suggested by lower levels of chitin accumulation in airways of aged wild-type mice and the inability to clear chitin in the context of human ILD and mice with telomere dysfunction. In the latter cases, chitin may be an environmental driver that contributes to the exacerbation of underlying disease induced by epithelial dysregulation. Intriguingly, lung fibrosis due to AMCase deficiency appears to initially activate gene pathways mediating epithelial integrity that have been previously implicated in the setting of lung fibrosis (Wolters et al., 2014; Sundar et al., 2015), suggesting that abnormal retention of chitin polymers in the airways instigates common epithelial stress pathways. For example, NRF2/glutathione-mediated oxidative stress responses in the lung are regulated by circadian rhythms (Pekovic-Vaughan et al., 2014), which can be disrupted during lung inflammation (Gibbs et al., 2014; Haspel et al., 2014), supporting that chitin particle-induced perturbations may instigate these same pathways in AMCase-deficient epithelial cells. In turn, epithelial dysfunction induced by unrelated means in aged individuals might also lead to increased retention of chitin polymers, perhaps by localized damage to epithelial cells that produce AMCase, impaired mucociliary clearance, or anatomic abnormalities, which all could contribute to the accumulation of chitin substrate beyond the degradative capacity of AMCase.

As established here using genetically deficient mice, AMCase is part of a nonredundant pathway for sustaining lung homeostasis, which is only apparent over time and in the presence of chitin substrate, perhaps reconciling other studies that have suggested a limited role for AMCase in lung pathologies (Vannella et al., 2016a; Fitz et al., 2012). ILD is similarly a disease that is related to aging, in which the capacity to mediate clearance of chitin, and potentially other particles, may be compromised. Notably, while protein levels of AMCase in airway fluid remained normal in the context of fibrotic disease, human BAL fluid endochitinase activity was, in general, comparatively lower than that of mouse, suggesting that chitin clearance in healthy humans may occur more slowly than in other species or rely more on mucociliary activity to efficiently clear the insoluble particles. Although we did not detect Chit1 protein in the airways, other secreted airway proteins such as surfactants, mucins, and enzymatically inactive chi-lectins have been associated with lung inflammation and fibrosis (Sutherland et al., 2014; Zhou et al., 2014; Wolters et al., 2014);

how these proteins might modulate or contribute to chitin-chitinase interactions in the airway lining fluid in health and disease remains to be unraveled. The expansion of chitin-binding chi-lectins at genetic loci where active chitinases reside in vertebrates (Hussain and Wilson, 2013) supports a model in which coordinate activities among these proteins are required to invade and process natural chitin-containing crystalline entities that impact in the lung, akin to the multi-component polysaccharide-processing proteins mobilized by bacteria to degrade cellulose (Smith and Bayer, 2013). Nevertheless, our findings that AMCase is the predominant chitinase in human BAL fluid and that chitin polymers accumulate in the lungs of patients with ILD raise the possibility that chitin constitutes an environmental driver that might contribute to the progression of lung diseases of diverse etiologies as normal epithelial function becomes compromised with age. Further studies will be necessary to reveal whether targeting this process might impact the course of these devastating diseases.

STAR ★ Methods

CONTACT FOR REAGENT AND RESOURCE SHARING

Further information and requests for resources and reagents should be directed to and will be fulfilled by the Lead Contact, Richard M. Locksley (richard.locksley@ucsf.edu).

EXPERIMENTAL MODEL AND SUBJECT DETAILS

Animal Studies—AMCase reporter mice (“ChiaRed”) were generated by homologous gene targeting in C57BL/6 embryonic stem cells, using a previously published cassette (Nussbaum et al., 2013), which contains (in order from 5′ to 3′) genomic sequence of the rabbit β-globin gene partial exon 2–3, the gene encoding tdTomato (Clontech), encephalomyocarditis virus IRES, humanized Cre recombinase, bovine growth hormone poly(A), and a *loxP*-flanked neomycin resistance cassette. Homologous arms flanking the *Chia1* translation initiation site (5′ arm: 2866 base pairs (bp); 3′ arm: 3081 bp) were amplified from C57BL/6 genomic DNA using Phusion polymerase (Finnzymes) and cloned into the cassette by standard methods. The construct was linearized with NotI and transfected by electroporation into C57BL/6 embryonic stem cells. Cells were grown on irradiated feeders with G418-containing media, and neomycin-resistant clones were screened for 5′ and 3′ homologous recombination by PCR and Southern blot. Two clones were selected for injection into albino C57BL/6 blastocysts to generate chimaeras, and males were bred with homozygous CMV-Cre transgenic C57BL/6 females [B6.C-Tg(CMV-Cre)1Cgn/J; The Jackson Laboratory] to excise the neomycin resistance cassette. Male and female C/+ heterozygous offspring were intercrossed to yield homozygous C/C ChiaRed mice. Primer sequences for genotyping ChiaRed mice were as follows: ChiaRed R (endogenous), 5′-GTGATGTGAGCTTAGAGAGCAAGA-3′, ChiaRed L2, 5′-GTCCTGACCACTTAGAAACCCTTA-3′; ChiaRed R2, 5′-CATGGTGATACAAGGGACATCTTC-3′. Previously described mice included SFTPC promoter-driven AMCase transgenic on BALB/c background (SPAM; Reese et al., 2007); this transgene was re-injected into pronuclei of fertilized C57BL/6 ChiaRed heterozygous eggs to generate SPAM ChiaRed mice. Other mice included BALB/c, C57BL/6 (The Jackson Laboratory), *Stat6*$^{-/-}$ (Kaplan et al., 1996), *Il4*$^{-/-}$*Il13*$^{-/-}$ (McKenzie et al., 1999), dual IFNγ/IL-17A (*ifng*$^{Great/Great}$*Il17a*$^{Smart/Smart}$; Price et al., 2012), IL-13 (*Il13*$^{Smart/Smart}$;

Liang et al., 2011) and IL-5 reporter (*Il5*$^{Red5/Red5}$; Nussbaum et al., 2013) strains. SFTPC-Cre^{ERT2} transgenic mice (Rock et al., 2011) were crossed with Trf1$^{flox/flox}$ mice (Martinez et al., 2009) to conditionally ablate TRF-1 in alveolar type II cells. Mice were maintained under specific pathogen-free conditions, fed ad libitum with irradiated PicoLab Rodent Diet 20 (LabDiet) and housed on PaperChip bedding material (Shepherd Specialty Papers). All animal protocols and procedures were approved by the University of California at San Francisco Institutional Animal Care and Use Committee.

Human Studies—Human BAL fluid was collected from patients with mild-to-moderate asthma (defined as airway hyper-responsiveness with PC_{20} to methacholine <= 8 mg/ml, and at least one of the following: asthma symptoms on at least two days per week, beta agonist use on at least two days per week, or FEV1 < 85% of predicted), ILD (diagnoses were made by inperson multidisciplinary team discussion (MDD) according to available guidelines) (Travis et al., 2013; van den Hoogen et al., 2013), and age-matched healthy controls (defined as no history of lung disease, normal spirometry; for asthma cohort, healthy was further defined as no history of allergic rhinitis, and absence of airway hyperresponsiveness to methacholine) (Table S3). All clinical studies were approved by the University of California at San Francisco Committee on Human Research, written informed consent was obtained from all subjects, and all studies were performed in accordance with the principles expressed in the Declaration of Helsinki.

METHOD DETAILS

***In vivo* treatments—**Mice were subcutaneously infected with 500 *Nippostrongylus brasiliensis* (*Nb*) third-stage larvae (L3) at the base of the tail, and euthanized at indicated time points for harvest of bronchalveoar lavage fluid (BAL), lung tissue, and small intestine. Recombinant mouse IL-13 (1 μg; Miltenyi) was administered intranasally to heterozygous ChiaRed mice (6–8 weeks of age) 48 hours before euthanasia and analysis, and recombinant mouse chitotriosidase (1 μg; R&D Systems) or vehicle (phosphate buffered saline; PBS) was administered intranasally every 2 days for 20 days to homozygous ChiaRed mice (12–16 months of age), which were euthanized 48 hours after the last dose for analysis of lung immune cells by flow cytometry and collagen content as described below. Intranasal challenges with *Aspergillus niger* hyphal preparation and purified chitin (New England Biolabs; NEB) were performed as described (Van Dyken et al., 2011; 2014). HDM preparations enriched for fecal pellets (318 fecal pellets : 28 mite bodies : 19 egg castings from *Dermatophagoides farinae;* Greer) were prepared and administered similarly. Blood oxygen saturation (SpO_2) was measured in anesthetized mice by pulse oxymetry (MouseOx Plus; Starr Life Sciences); average values from two separate readings on consecutive days were recorded per animal.

Chitinase assays—BAL fluid (10 μl) was incubated for 1 hour at 37°C, pH 5.0, protected from light, in the presence of 4-methylumbelliferyl-N-acetyl-β-D-glucosaminide, 4-methylumbelliferyl-N,N′-diacetyl-β-D-chitobioside, or 4-methylumbelliferyl-β-D-N,N′,N″-triacetylchitotriose substrates (0.5 mg/ml; Sigma) in 100 μl final volume assay buffer, for evaluation of β-N-glucosaminidase, chitobiosidase, or chitotriosidase activities, respectively. Reactions were stopped with sodium carbonate buffer and fluorescent signal was quantified

using a FlexStation 3 (excitation 360 nm/emission 450 nm; Molecular Devices). Relative activity measurements were calculated after subtracting background values from wells containing substrate alone using a standard curve generated with serial dilutions of 4-methylumbelliferone. Chitinase from *Trichoderma viride* (Sigma) was used as a positive control and results from duplicate wells were averaged for all samples.

Tissue preparation and cell sorting—Human BAL fluid was obtained using the standard approach (Goldstein et al., 1990) in a single sub-segment of either the right middle lobe or the lingula, with a total of 100 mL (for ILD cohort) or 200 ml (for asthma cohort) of sterile saline instilled, and similar returns among subject groups; analytes were normalized by volume. The BAL fluid was kept on ice and processed within 1 h of collection, then frozen at −80° C until analysis. Mouse BAL fluid was collected by intratracheal installation of 1 ml sterile PBS, which was centrifuged for 5 min at 1600 rpm. Supernatants were removed and analyzed for chitinase activity, while the remaining 100 μl was heat-treated at 95 °C with intermittent shaking for 20 min, to lyse cellular material and denature protein elements prior to assaying for chitin content. Whole lungs were perfused with 20 ml PBS via heart puncture before preparing single-cell suspensions with an automated tissue dissociator (gentleMACS; Miltenyi Biotec).

For enumeration of lung immune infiltrates by flow cytometry, cells were prepared as described previously (Van Dyken et al., 2014), using antibodies listed in Key Resources and gating as described in Figure S1C. For cell sorting and analysis of lung epithelial populations, cells were prepared by intratracheally instilling 2 ml dispase II (5 mg/ml, pre-warmed to 37° C) followed by instillation of 0.5 ml low-melting point agarose (ThermoFisher; 0.1% w/v in HBSS, pre-warmed) into lungs in situ, which were covered with a Kimwipe (Fisher) and cooled with ice for 1 minute. The lungs were removed from the chest cavity, placed in 2 ml dispase II (5 mg/ml), incubated at room temperature for 45 minutes, then transferred to C tubes (Miltenyi) containing 5 ml DNase I solution (Roche; 25 μg/ml in HBSS). The lungs were dissociated by running gentleMACS program lung_01, then incubating at room temperature for 10 minutes with agitation, followed by program lung_02. The tissue was further dispersed by passing through 70 μm nylon filters, washed, and subjected to red blood cell lysis (PharmLyse; BD Biosciences) before final suspension and staining in PBS with 2% fetal calf serum for flow cytometry. Exclusion of DAPI (4′,6-diamidine-2′-phenylindole dihydrochloride; Roche) identified live cells, which were enumerated with flow cytometric counting beads (CountBright Absolute; Life Technologies). Sample data were acquired using BD FACSDiva with a 4-laser LSRII or Fortessa flow cytometer (BD Biosciences) and analyzed using FlowJo software (Tree Star, Inc.). CD45-DAPI-EpCAM+ epithelial cells expressing the ChiaRed reporter as indicated were sorted to >95% purity using a MoFlo XDP (Beckman Coulter).

Quantitative RT-PCR—Total RNA was extracted from lung tissue as described (Mohapatra et al., 2016). For sorted cells, alveolar macrophages (CD45+CD3-Thy1.2-CD11b-CD11c+Siglec F+) or epithelial cells (CD45-CD3-Thy1.2-CD11b-CD11c-Siglec F-EpCAM+) were lysed in RLT Plus and total RNA was eluted from RNeasy Plus Micro columns as recommended (Qiagen). RNA concentration and purity was assessed with a

spectrophotometer (NanoDrop; ThermoFisher) and equal amounts of total RNA were reverse transcribed with VILO cDNA Synthesis Kit prior to quantitative PCR (using ΔΔCt) using the Power SYBR Green reagent on a StepOnePlus cycler (ThermoFisher). Primer sequences: *18s*, 5′ -GAAACGGCTACCACATCCAAG-3′, 5′ -TTACAGGGCCTCGAAAGAGTC-3′ ; *Chia1*, 5′ -TACCAGACAGGCTGGGTTCT-3′, 5′ -GGAGTAGTCACTGGCTCGGA-3′; *Chit1*, 5′ -GGCATAACAGCCCCCTCTAC-3′, 5′ -TGAAGCTTTCCACGTCGTCA-3′ ; *Ovgp1*, 5′ -CACTTGCCAACCGGGAAAAG-3′, 5′ -GTTTATCTGCGGGTGTCCCA-3′ ; *Chil1*, 5′ -TTACCAGACGCCATCCAACC-3′, 5′ -TGACAGGTGCCCTGGAAATC-3′; *Chil3*, 5′ -CCTGCCTGTGTACTCACCTG-3′, 5′ -GCAGCCTTGGAATGTCTTTCT-3′; *Chil4*, 5′ -ACCACATTCCAAGGCTGCTAC-3′, 5′ -CCCTCGATAAGAGGCCTTGC-3′;*Chil5*, 5′-CGGAAGGAAGGGATGTGTGG-3′, 5′-GCAGAAGTGCCAAACCTGTG-3′; *Chil6*, 5′-CACTCCTGAGAACCGCCATT-3′, 5′-GTTTGCTTTGTGTGGGGTCC-3′.

RNA-Seq—Epithelial cells (approximately 110,000 cells per mouse) were sorted from the lungs of 14 week-old wild-type (CD45-DAPI-EpCAM+) or ChiaRed homozygous and heterozygous reporter mice (CD45-DAPI-EpCAM+ChiaRed+), lysed in RLT media and processed using the miRNeasy Micro kit with on-column DNAse treatment (Qiagen). Total RNA quality was assessed by NanoDrop (Thermo) and the Agilent 2100 Bioanalyzer (Agilent Technologies). RNA sequencing libraries were generated using the Illumina TruSeq stranded mRNA kit, according to the manufacturer's protocol (Illumina). Library fragment size distributions were assessed using the Bioanalyzer 2100 and the DNA high-sensitivity chip. Library concentrations were measured using KAPA Library Quantification Kits (Kapa Biosystems), and equal amounts of indexed libraries were pooled and sequenced on the HiSeq 4000 (Illumina) from which ~1.5 billion reads were obtained with an average read depth of 74.1 million reads/sample. Sequence alignment and splice junction estimation was performed using STAR (Dobin et al., 2013). Mappings were restricted to those that were uniquely assigned to the mouse transcriptome, as provided by Ensembl (Flicek, et al., 2014) and aggregated on a pergene basis. These raw data were analyzed using DESeq2 (Anders and Huber, 2010) to assess variance and differential expression among all sorted epithelial cell samples (n = 18); specific comparisons shown in Fig. 1 and Fig. 7 represent averages calculated from biological replicates (wild-type, n = 3; ChiaRed homozygous, n = 2; ChiaRed heterozygous, n = 3). Among differentially expressed genes (false discovery rate < 0.05), 1463 genes that were expressed at a level of > 100 fragments per kilobase of exon per million mapped reads (FPKM) in either one of the cell populations were evaluated for pathway enrichment by Fisher's exact text right-tailed using Inginuity Pathway Analysis software (Qiagen).

Protein and chitin assays—BAL fluid (10 μl) proteins were separated by SDS-PAGE, transferred to PVDF membranes, probed with polyclonal anti-human/mouse AMCase (Abcam) or anti-human or anti-mouse Chitl (R&D Systems), followed by biotinylated IgG secondary antibodies and streptavidin-HRP (Vector). Recombinant human or mouse Chitl (R&D) and recombinant mouse AMCase (Reese et al., 2007) were used as positive controls. Standard ELISA was performed to determine levels of mouse Yml protein in BAL fluid (R&D) and serum IgG1 (eBioscience) and IgE (BioLegend). Detection of chitin in BAL

fluid was performed for each sample in duplicate using a previously described dot-blot assay (Van Dyken et al., 2011). Briefly, 1 μl of BAL fluid was placed onto nitrocellulose membranes (GE Healthcare). Sonicated chitin (Sigma) was used as a positive control to generate a standard curve, from which relative values for each sample were calculated in order to compare separate blots. The membranes were covered and dried overnight at room temperature, rinsed in tris-buffered saline containing 0.05% Tween-20 (TBST), blocked with 5% bovine serum albumin (BSA) in TBST, and incubated with FITC-chitin-binding domain probe (CBD; New England Biolabs) in 1% BSA/TBST for 16 hrs at 4° C with gentle rocking. After washing with TBST, the membranes were incubated with HRP-anti-fluorescein (Perkin Elmer) for 45 min at room temperature, washed and developed with ECL substrate (Thermo Scientific). Data from blots were acquired and analyzed with a ChemiDoc MP and Image Lab 5.1 software (BioRad). For hydroxyproline assays, snap-frozen whole lung tissue (10 mg) was homogenized in M tubes (Miltenyi) containing ice-cold ultrapure water (0.1 ml) by running gentleMACS program Protein_01 twice. Concentrated hydrochloric acid (12 M; 0.1 ml) was added, and samples were hydrolyzed for 3 hrs at 120°C. Supernatants (50 μl) were transferred to 96-well microplates and wells were evaporated to dryness by incubating at 60°C for 20 hrs. The concentration of hydroxyproline was determined by the reaction of oxidized hydroxyproline with 4-(dimethylamino)-benzaldehyde as recommended by the manufacturer (Sigma), measuring absorbance at 560 nm using a SpectraMax spectrophotometer (Molecular Devices).

Histology—For immunohistochemical staining of tdTomato in ChiaRed lungs, samples were fixed in 4% paraformaldehyde, immersed in 30% sucrose, and embedded in OCT compound (Sakura Finetek) prior to frozen sectioning at 6 μm using a Leica CM 3050S cryomicrotome (Leica Microsystems). Amplification of tdTomato fluorescence in ChiaRed mice was achieved using polyclonal anti-dsRed (Clontech) followed by anti-rabbit-A555 (Thermo), and in combination with anti-EpCAM-AF488 (BioLegend), anti-SPC-FITC (LSBio), or anti-Foxj1 (eBioscience) using mouse blocking reagent (Vector). Masson's trichrome stain was performed by the UCSF Anatomic Pathology Clinical Laboratory on paraffin-embedded lungs fixed in 4% paraformaldehyde. Images were acquired with an AxioCam HRm camera and AxioImager M2 upright microscope (Carl Zeiss).

QUANTIFICATION AND STATISTICAL ANALYSIS

Statistical analysis—Statistical analysis for RNA-seq data is described above. Data in all figures represent mean ± S.E.M. unless otherwise indicated, and results from independent experiments were pooled when possible. Data were analyzed using Prism (GraphPad, Inc.), using unpaired two-tailed Student's *t* tests; significance was defined as indicated in figure legends.

DATA AND SOFTWARE AVAILABILITY

Accession codes—RNA-Seq data have been deposited in NCBI's GENE Expression Omnibus and are accessible through GEO Series.

KEY RESOURCES TABLE

REAGENT or RESOURCE	SOURCE	IDENTIFIER
Antibodies		
Anti-mouse CD11c PE/Cy7 (clone N418)	BioLegend	Cat# 117318
Anti-mouse CD11c BV785 (clone N418)	BioLegend	Cat# 117336
Anti-mouse/human CD11b AF647 (clone M1/70)	BioLegend	Cat# 101218
Anti-mouse/human CD11b BV650 (clone M1/70)	BioLegend	Cat# 101259
Anti-mouse TCRγδ PerCP/Cy5.5 (clone GL3)	BioLegend	Cat# 118118
Anti-mouse CD3ε PE/Cy7 (clone 17A2)	BioLegend	Cat# 100220
Anti-mouse CD3ε AF647 (clone 17A2)	BioLegend	Cat# 100209
Anti-mouse CD69 FITC (clone H1.2F3)	BioLegend	Cat# 104506
Anti-mouse CD69 PE (clone H1.2F3)	BioLegend	Cat# 104508
Anti-mouse CD4 BV605 (clone RM4-5)	BioLegend	Cat# 100548
Anti-mouse CD4 BV711 (clone RM4-5)	BioLegend	Cat# 100550
Anti-mouse CD8α BV605 (clone 53–6.7)	BioLegend	Cat# 100744
Anti-mouse CD25 APC/Cy7 (clone PC61)	BioLegend	Cat# 102026
Anti-mouse CD25 PerCP/Cy5.5 (clone PC61)	BioLegend	Cat# 102030
Anti-mouse CD326 AF488 (clone G8.8)	BioLegend	Cat# 118210
Anti-mouse CD326 APC (clone G8.8)	BioLegend	Cat# 118214
Anti-mouse CD326 BV605 (clone G8.8)	BioLegend	Cat# 118227
Anti-mouse NK1.1 PerCP/Cy5.5 (clone PK136)	BioLegend	Cat# 108728
Anti-mouse Thy1.2 BV605 (clone 53–2.1)	BioLegend	Cat# 140318
Anti-mouse CD200 APC (clone OX-90)	BioLegend	Cat# 123810
Anti-mouse Ly6G APC/Cy7 (clone 1A8)	BioLegend	Cat# 127624
Anti-mouse Ly6G APC (clone 1A8)	BioLegend	Cat# 127614
Anti-human CD271 PE (ME20.4)	BioLegend	Cat# 345106
Anti-human CD271 APC (ME20.4)	BioLegend	Cat# 345108
Anti-human CD4 PE (RPA-T4)	eBioscience	Cat# 12-0049
Anti-human CD4 APC (RPA-T4)	eBioscience	Cat# 17-0049
Anti-mouse KLRG1 PerCP-eF710 (clone 2F1)	eBioscience	Cat# 17-5893
Anti-mouse CD49b APC (clone DX5)	eBioscience	Cat# 17-5971
Anti-mouse CD49b eF450 (clone DX5)	eBioscience	Cat# 48-5971
Anti-mouse/human FOXJ1 (clone 2A5)	eBioscience	Cat# 14-9965
Anti-mouse CD45 BUV395 (clone 30-F11)	BD Biosciences	Cat# 565967
Anti-mouse CD45 APC/Cy7 (clone 30-F11)	BD Biosciences	Cat# 561037
Anti-mouse CD45 BV711 (clone 30-F11)	BD Biosciences	Cat# 563709
Anti-mouse Siglec F AF647 (clone E50-2440)	BD Biosciences	Cat# 562680
Anti-mouse Siglec F BB515 (clone E50-2440)	BD Biosciences	Cat# 564514
Anti-mouse TCR Vp FITC screening panel	BD Biosciences	Cat# 557004

REAGENT or RESOURCE	SOURCE	IDENTIFIER
Anti-human/mouse AMCase, rabbit polyclonal	abcam	Cat# ab72309
Anti-human chitotriosidase/Chit1, goat polyclonal	R&D Systems	Cat# AF3559
Anti-mouse chitotriosidase/Chit1, sheep polyclonal	R&D Systems	Cat# AF5325
Goat Anti-Rabbit IgG (H+L), Mouse/Human ads-HRP	SouthernBiotech	Cat# 4050-05
Rabbit Anti-Sheep IgG (H+L)-HRP	SouthernBiotech	Cat# 6150-05
Rabbit Anti-Goat IgG (H+L)-HRP	SouthernBiotech	Cat# 6160-05
Anti-fluorescein-HRP	Perkin Elmer	Cat# NEF710001 EA
Anti-DsRed, rabbit polyclonal	Clontech	Cat# 632496
Goat anti-Rabbit IgG (H+L)-AF555	ThermoFisher	Cat# A-21428
Anti-mouse/human SFTPC-FITC, rabbit polyclonal	LSBio	Cat# LS-C442308
Biological Samples		
Human bronchoalveolar lavage fluid, healthy, IPF, SSc	UCSF (P. Wolters)	N/A
Human bronchoalveolar lavage fluid, healthy, asthma	UCSF (P. Woodruff)	N/A
Aspergillus niger hyphal preparation	Van Dyken et al., 2011	N/A
Dermatophagoides farina fecal preparation	Greer	N/A
Chemicals, Peptides, and Recombinant Proteins		
Recombinant mouse chitotriosidase, low endotoxin	R&D Systems	Custom bulk prep.
Recombinant mouse AMCase	Reese et al., 2007	N/A
Recombinant mouse IL-13	Miltenyi Biotec	Cat# 130-094
Chitin binding domain probe-FITC	New England Biolabs	Cat# P5211
Chitinase from *Trichoderma viride*	Sigma	Cat# C8241
RNeasy plus micro kit	Qiagen	Cat# 74034
miRNeasy micro kit	Qiagen	Cat# 217084
Superscript VILO cDNA synthesis kit	ThermoFisher	Cat# 11754050
Power SYBR Green PCR master mix	ThermoFisher	Cat# 4368706
TruSeq stranded mRNA library prep kit	Illumina	Cat# RS-122
KAPA library quantification kit	Kapa Biosystems	Cat# KK4824
Critical Commercial Assays		
Fluorimetric chitinase assay	Sigma	Cat# CS1030
Hydroxyproline assay	Sigma	Cat# MAK008
Mouse on mouse blocking reagent	Vector	Cat# MKB-2213
Mouse Ym1/Chi3l3 ELISA	R&D Systems	Cat# DY2446
Mouse IgE ELISA	BioLegend	Cat# 432401
Mouse IgG_1 ELISA	eBioscience	Cat# 88-50410

REAGENT or RESOURCE	SOURCE	IDENTIFIER
Deposited Data		
RNA-Seq data	This study	NCBI GEO:
Experimental Models: Cell Lines		
Experimental Models: Organisms/Strains		
Mouse: C57BL/6J	The Jackson Laboratory	Cat# 000664
Mouse: C57BL/6J *Chia1*^{ChiaRed}	This study	N/A
Mouse: C57BL/6J SPAM^{Tg}*Chia1*$^{ChiaRed/ChiaRed}$	This study	N/A
Mouse: BALB/c SPAM^{Tg}	Reese et al., 2007	N/A
Mouse: BALB/c	The Jackson Laboratory	Cat# 000651
Mouse: BALB/c SPAM^{Tg}	Reese et al., 2007	N/A
Mouse: C57BL/6J *Stat6*$^{-/-}$	Kaplan et al., 1996	N/A
Mouse: C57BL/6J *114*$^{-/-}$ *113*$^{-/-}$	McKenzie et al., 1999	N/A
Mouse: C57BL/6J *Ifng*$^{Great/Great}$*Il17a*$^{Smart/Smart}$	Price et al., 2012	N/A
Mouse: C57BL/6J *Il13*$^{Smart/Smart}$	Liang et al., 2011	N/A
Mouse: C57BL/6J *Il5*$^{Red5/Red5}$	Nussbaum et al., 2013	N/A
Mouse: C57BL/6J *Sftpc*^{CreER12}	Rock et al., 2011	N/A
Mouse: C57BL/6J *Trf1*$^{flox/flox}$	Martinez et al., 2009	N/A
Nippostrongy/us brasi/iensis	UCSF (R. Locksley)	N/A
Oligonucleotides		
Recombinant DNA		
Software and Algorithms		
FlowJo v.10.0	FlowJo	www.flowjo.com
Prism v.6.0	GraphPad	www.graphpad.com
Ingenuity Pathway Analysis v.01-07	Qiagen	www.qiagenbioinformatics.com
STAR	Dobin et al., 2013	https://github.com/alexdobin/STAR
DESeq2	Anders and Huber, 2010	https://bioconductor.org/packages/release/bioc/html/DESeq2.html
ImageLab v.5.1	BioRad	www.biorad.com
Other		

Supplementary Material

Refer to Web version on PubMed Central for supplementary material.

Acknowledgments

We thank A. Abbas, J. Fraser and D. Sheppard for comments on the manuscript, D. Corry and D. Voehringer for reagents, Z. Wang, K. Davis, M. Ji and M. Consengco for expert technical assistance, C. Nguyen and J. La for assistance with clinical studies, and Josh Pollack and staff at the UCSF Functional Genomics Core Facility for assistance with RNA-Seq. This work was supported by grants AI30663, AI26918, HL128903 and HL107202 from the National Institutes of Health, Howard Hughes Medical Institute, Nina Ireland Program for Lung Health, and the Sandler Asthma Basic Research Center at the University of California, San Francisco.

References

Adrangi S, Faramarzi MA. From bacteria to human: a journey into the world of chitinases. Biotechnol Adv. 2008; 31:1786–1795.

Aminuddin F, Akhabir L, Stefanowicz D, Pare PD, Connett JE, Anthonisen NR, Fahy JV, Seibold MA, Burchard EG, Eng C, et al. Genetic association between human chitinases and lung function in COPD. Hum Genet. 2012; 131:1105–1114. [PubMed: 22200767]

Anders S, Huber W. Differential expression analysis for sequence count data. Genome Biol. 2010; 11:R106. [PubMed: 20979621]

Dobin A, Davis CA, Schlesinger F, Drenkow J, Zaleski C, Jha S, Batut P, Chaisson M, Gingeras TR. STAR: ultrafast universal RNA-seq aligner. Bioinformatics. 2013; 29:15–21. [PubMed: 23104886]

Finkelman FD, Madden KB, Cheever AW, Katona IM, Morris SC, Gately MK, Hubbard BR, Gause WC, Urban JF. Effects of interleukin 12 on immune responses and host protection in mice infected with intestinal nematode parasites. J Exp Med. 1994; 179:1563–1572. [PubMed: 7909327]

Fitz LJ, DeClercq C, Brooks J, Kuang W, Bates B, Demers D, Winkler A, Nocka K, Jiao A, Greco RM, et al. Acidic mammalian chitinase is not a critical target for allergic airway disease. Am J Respir Cell Mol Biol. 2012; 46:71–79. [PubMed: 21836154]

Flicek P, Amode MR, Barrell D, Beal K, Billis K, Brent S, Carvalho-Silva D, Clapham P, Coates G, Fitzgerald S, et al. Ensembl 2014. Nucleic Acids Res. 2014; 42:D749–55. [PubMed: 24316576]

Gibbs J, Ince L, Matthews L, Mei J, Bell T, Yang N, Saer B, Begley N, Poolman T, Pariollaud M, et al. An epithelial circadian clock controls pulmonary inflammation and glucocorticoid action. Nat Med. 2014; 20:919–926. [PubMed: 25064128]

Goedken ER, O'Brien RF, Xiang T, Banach DL, Marchie SC, Barlow EH, Hubbard S, Mankovich JA, Jiang J, Richardson PL, et al. Functional comparison of recombinant acidic mammalian chitinase with enzyme from murine bronchoalveolar lavage. Protein Expr Purif. 2011; 75:55–62. [PubMed: 20826216]

Goldstein RA, Rohatgi PK, Bergofsky EH, Block ER, Daniele RP, Dantzker DR, Davis GS, Hunninghake GW, King TEJ, Metzger WJ. Clinical role of bronchoalveolar lavage in adults with pulmonary disease. Am Rev Respir Dis. 1990; 142:481–486. [PubMed: 2200319]

Hams E, Armstrong ME, Barlow JL, Saunders SP, Schwartz C, Cooke G, Fahy RJ, Crotty TB, Hirani N, Flynn RJ, et al. IL-25 and type 2 innate lymphoid cells induce pulmonary fibrosis. Proc Natl Acad Sci U S A. 2014; 111:367–372. [PubMed: 24344271]

Haspel JA, Chettimada S, Shaik RS, Chu JH, Raby BA, Cernadas M, Carey V, Process V, Hunninghake GM, Ifedigbo E, et al. Circadian rhythm reprogramming during lung inflammation. Nat Commun. 2014; 5:4753. [PubMed: 25208554]

Hübner RH, Gitter W, El Mokhtari NE, Mathiak M, Both M, Bolte H, Freitag-Wolf S, Bewig B. Standardized quantification of pulmonary fibrosis in histological samples. Biotechniques. 2008; 44:507–511–517. [PubMed: 18476815]

Hussain M, Wilson JB. New paralogues and revised time line in the expansion of the vertebrate GH18 family. J Mol Evol. 2013; 76:240–260. [PubMed: 23558346]

Kaplan MH, Schindler U, Smiley ST, Grusby MJ. Stat6 is required for mediating responses to IL-4 and for development of Th2 cells. Immunity. 1996; 4:313–319. [PubMed: 8624821]

Karo-Atar D, Bordowitz A, Wand O, Pasmanik-Chor M, Fernandez IE, Itan M, Frenkel R, Herbert DR, Finkelman FD, Eickelberg O, et al. A protective role for IL-13 receptor alpha 1 in bleomycin-induced pulmonary injury and repair. Mucosal Immunol. 2016; 9:240–253. [PubMed: 26153764]

Keyhani NO, Roseman S. Physiological aspects of chitin catabolism in marine bacteria. Biochim Biophys Acta. 1999; 1473:108–122. [PubMed: 10580132]

Kim LK, Morita R, Kobayashi Y, Eisenbarth SC, Lee CG, Elias J, Eynon EE, Flavell RA. AMCase is a crucial regulator of type 2 immune responses to inhaled house dust mites. Proc Natl Acad Sci U S A. 2015; 112:E2891–9. [PubMed: 26038565]

Kotton DN, Morrisey EE. Lung regeneration: mechanisms, applications and emerging stem cell populations. Nat Med. 2014; 20:822–832. [PubMed: 25100528]

Liang HE, Reinhardt RL, Bando JK, Sullivan BM, Ho IC, Locksley RM. Divergent expression patterns of IL-4 and IL-13 define unique functions in allergic immunity. Nat Immunol. 2011; 13:58–66. [PubMed: 22138715]

Manno N, Sherratt S, Boaretto F, Coico FM, Camus CE, Campos CJ, Musumeci S, Battisti A, Quinnell RJ, Leon JM, et al. High prevalence of chitotriosidase deficiency in Peruvian Amerindians exposed to chitin-bearing food and enteroparasites. Carbohydr Polym. 2014; 113:607–614. [PubMed: 25256524]

Martinez P, Thanasoula M, Munoz P, Liao C, Tejera A, McNees C, Flores JM, Fernandez-Capetillo O, Tarsounas M, Blasco MA. Increased telomere fragility and fusions resulting from TRF1 deficiency lead to degenerative pathologies and increased cancer in mice. Genes Dev. 2009; 23:2060–2075. [PubMed: 19679647]

McKenzie GJ, Fallon PG, Emson CL, Grencis RK, McKenzie AN. Simultaneous disruption of interleukin (IL)-4 and IL-13 defines individual roles in T helper cell type 2-mediated responses. J Exp Med. 1999; 189:1565–1572. [PubMed: 10330435]

Mohapatra A, Van Dyken SJ, Schneider C, Nussbaum JC, Liang HE, Locksley RM. Group 2 innate lymphoid cells utilize the IRF4-IL-9 module to coordinate epithelial cell maintenance of lung homeostasis. Mucosal Immunol. 2015; 9:275–286. [PubMed: 26129648]

Naikawadi RP, Disayabutr S, Mallavia B, Donne ML, Green G, La JL, Rock JR, Looney MR, Wolters PJ. Telomere dysfunction in alveolar epithelial cells causes lung remodeling and fibrosis. JCI Insight. 2016; 1:e86704. [PubMed: 27699234]

Nussbaum JC, Van Dyken SJ, von Moltke J, Cheng LE, Mohapatra A, Molofsky AB, Thornton EE, Krummel MF, Chawla A, Liang HE, et al. Type 2 innate lymphoid cells control eosinophil homeostasis. Nature. 2013; 502:245–248. [PubMed: 24037376]

Okawa K, Ohno M, Kashimura A, Kimura M, Kobayashi Y, Sakaguchi M, Sugahara Y, Kamaya M, Kino Y, Bauer PO, et al. Loss and gain of human acidic mammalian chitinase activity by non-synonymous SNPs. Mol Biol Evol. 2016; 33:3183–3193. [PubMed: 27702777]

Pekovic-Vaughan V, Gibbs J, Yoshitane H, Yang N, Pathiranage D, Guo B, Sagami A, Taguchi K, Bechtold D, Loudon A, et al. The circadian clock regulates rhythmic activation of the NRF2/glutathionemediated antioxidant defense pathway to modulate pulmonary fibrosis. Genes Dev. 2014; 28:548–560. [PubMed: 24637114]

Povedano JM, Martinez P, Flores JM, Mulero F, Blasco MA. Mice with pulmonary fibrosis driven by telomere dysfunction. Cell Rep. 2015; 12:286–299. [PubMed: 26146081]

Price AE, Reinhardt RL, Liang HE, Locksley RM. Marking and quantifying IL-17A-producing cells in vivo. PLoS One. 2012; 7:e39750. [PubMed: 22768117]

Reese TA, Liang HE, Tager AM, Luster AD, Van Rooijen N, Voehringer D, Locksley RM. Chitin induces accumulation in tissue of innate immune cells associated with allergy. Nature. 2007; 447:92–96. [PubMed: 17450126]

Rock JR, Barkauskas CE, Cronce MJ, Xue Y, Harris JR, Liang J, Noble PW, Hogan BLM. Multiple stromal populations contribute to pulmonary fibrosis without evidence for epithelial to mesenchymal transition. Proc Natl Acad Sci. 2011; 108:E1475–E1483. [PubMed: 22123957]

Rockey DC, Bell PD, Hill JA. Fibrosis — a common pathway to organ injury and Failure. N Engl J Med. 2015; 372:1138–1149. [PubMed: 25785971]

Salo PM, Arbes SJ, Jaramillo R, Calatroni A, Weir CH, Sever ML, Hoppin JA, Rose KM, Liu AH, Gergen PJ, et al. Prevalence of allergic sensitization in the United States: Results from the National Health and Nutrition Examination Survey (NHANES) 2005-2006. J Allergy Clin Immunol. 2014; 134:350–359. [PubMed: 24522093]

Schimpl M, Rush CL, Betou M, Eggleston IM, Recklies AD, van Aalten DMF. Human YKL-39 is a pseudo-chitinase with retained chitooligosaccharide-binding properties. Biochem J. 2012; 446:149–157. [PubMed: 22742450]

Schwartzman JA, Koch E, Heath-Heckman EAC, Zhou L, Kremer N, McFall-Ngai MJ, Ruby EG. The chemistry of negotiation: rhythmic, glycan-driven acidification in a symbiotic conversation. Proc Natl Acad Sci U S A. 2015; 112:566–571. [PubMed: 25550509]

Seibold MA, Reese TA, Choudhry S, Salam MT, Beckman K, Eng C, Atakilit A, Meade K, Lenoir M, Watson HG, et al. Differential enzymatic activity of common haplotypic versions of the human acidic mammalian chitinase protein. J Biol Chem. 2009; 284:19650–19658. [PubMed: 19435888]

Smith SP, Bayer EA. Insights into cellulosome assembly and dynamics: from dissection to reconstruction of the supramolecular enzyme complex. Curr Opin Struct Biol. 2013; 23:686–694. [PubMed: 24080387]

Sundar IK, Yao H, Sellix MT, Rahman I. Circadian molecular clock in lung pathophysiology. Am J Physiol -Lung Cell Mol Physiol. 2015; 309:L1056–L1075. [PubMed: 26361874]

Sutherland TE, Logan N, Ruckerl D, Humbles AA, Allan SM, Papayannopoulos V, Stockinger B, Maizels RM, Allen JE. Chitinase-like proteins promote IL-17-mediated neutrophilia in a tradeoff between nematode killing and host damage. Nat Immunol. 2014; 15:1116–1125. [PubMed: 25326751]

Travis WD, Costabel U, Hansell DM, King TE, Lynch DA, Nicholson AG, Ryerson CJ, Ryu JH, Selman M, Wells AU, et al. An official American Thoracic Society/European Respiratory Society statement: Update of the international multidisciplinary classification of the idiopathic interstitial pneumonias. Am J Respir Crit Care Med. 2013; 188:733–748. [PubMed: 24032382]

van den Hoogen F, Khanna D, Fransen J, Johnson SR, Baron M, Tyndall A, Matucci-Cerinic M, Naden RP, Medsger TAJ, Carreira PE, et al. 2013 classification criteria for systemic sclerosis: an American College of Rheumatology/European League against Rheumatism collaborative initiative. Arthritis Rheum. 2013; 65:2737–2747. [PubMed: 24122180]

Van Dyken SJ, Garcia D, Porter P, Huang X, Quinlan PJ, Blanc PD, Corry DB, Locksley RM. Fungal chitin from asthma-associated home environments induces eosinophilic lung infiltration. J Immunol. 2011; 187:2261–2267. [PubMed: 21824866]

Van Dyken SJ, Mohapatra A, Nussbaum JC, Molofsky AB, Thornton EE, Ziegler SF, McKenzie ANJ, Krummel MF, Liang HE, Locksley RM. Chitin activates parallel immune modules that direct distinct inflammatory responses via innate lymphoid type 2 and γδ T cells. Immunity. 2014; 40:414–424. [PubMed: 24631157]

Van Dyken SJ, Nussbaum JC, Lee J, Molofsky AB, Liang HE, Pollack JL, Gate RE, Haliburton GE, Ye CJ, Marson A, et al. A tissue checkpoint regulates type 2 immunity. Nat Immunol. 2016; 17:1381–1387. [PubMed: 27749840]

Vannella KM, Ramalingam TR, Hart KM, de Queiroz Prado R, Sciurba J, Barron L, Borthwick LA, Smith AD, Mentink-Kane M, White S, et al. Acidic chitinase primes the protective immune response to gastrointestinal nematodes. Nat Immunol. 2016a; 17:538–544. [PubMed: 27043413]

Vannella KM, Ramalingam TR, Borthwick LA, Barron L, Hart KM, Thompson RW, Kindrachuk KN, Cheever AW, White S, Budelsky AL, et al. Combinatorial targeting of TSLP, IL-25, and IL-33 in type 2 cytokine-driven inflammation and fibrosis. Sci Transl Med. 2016b; 8:337ra65.

Watanabe T, Ito Y, Yamada T, Hashimoto M, Sekine S, Tanaka H. The roles of the C-terminal domain and type III domains of chitinase A1 from Bacillus circulans WL-12 in chitin degradation. J Bacteriol. 1994; 176:4465–4472. [PubMed: 8045877]

Wilson MS, Madala SK, Ramalingam TR, Gochuico BR, Rosas IO, Cheever AW, Wynn TA. Bleomycin and IL-1beta-mediated pulmonary fibrosis is IL-17A dependent. J Exp Med. 2010; 207:535–552. [PubMed: 20176803]

Wolters PJ, Collard HR, Jones KD. Pathogenesis of idiopathic pulmonary fibrosis. Annu Rev Pathol. 2014; 9:157–179. [PubMed: 24050627]

Zhou Y, Peng H, Sun H, Peng X, Tang C, Gan Y, Chen X, Mathur A, Hu B, Slade MD, et al. Chitinase 3-like 1 suppresses injury and promotes fibroproliferative responses in mammalian lung fibrosis. Sci Transl Med. 2014; 6:240ra76.

Zhu Z, Zheng T, Homer RJ, Kim YK, Chen NY, Cohn L, Hamid Q, Elias JA. Acidic mammalian chitinase in asthmatic Th2 inflammation and IL-13 pathway activation. Science. 2004; 304:1678–1682. [PubMed: 15192232]

HIGHLIGHTS

- AMCase-expressing epithelial cells mediate endochitinase activity in the airways
- Environmental chitin spontaneously accumulates in airways lacking AMCase
- Persistent immune activation and age-related fibrosis develop in the absence of AMCase
- Mice with fibrotic lung disease and humans with ILD accumulate chitin in airways

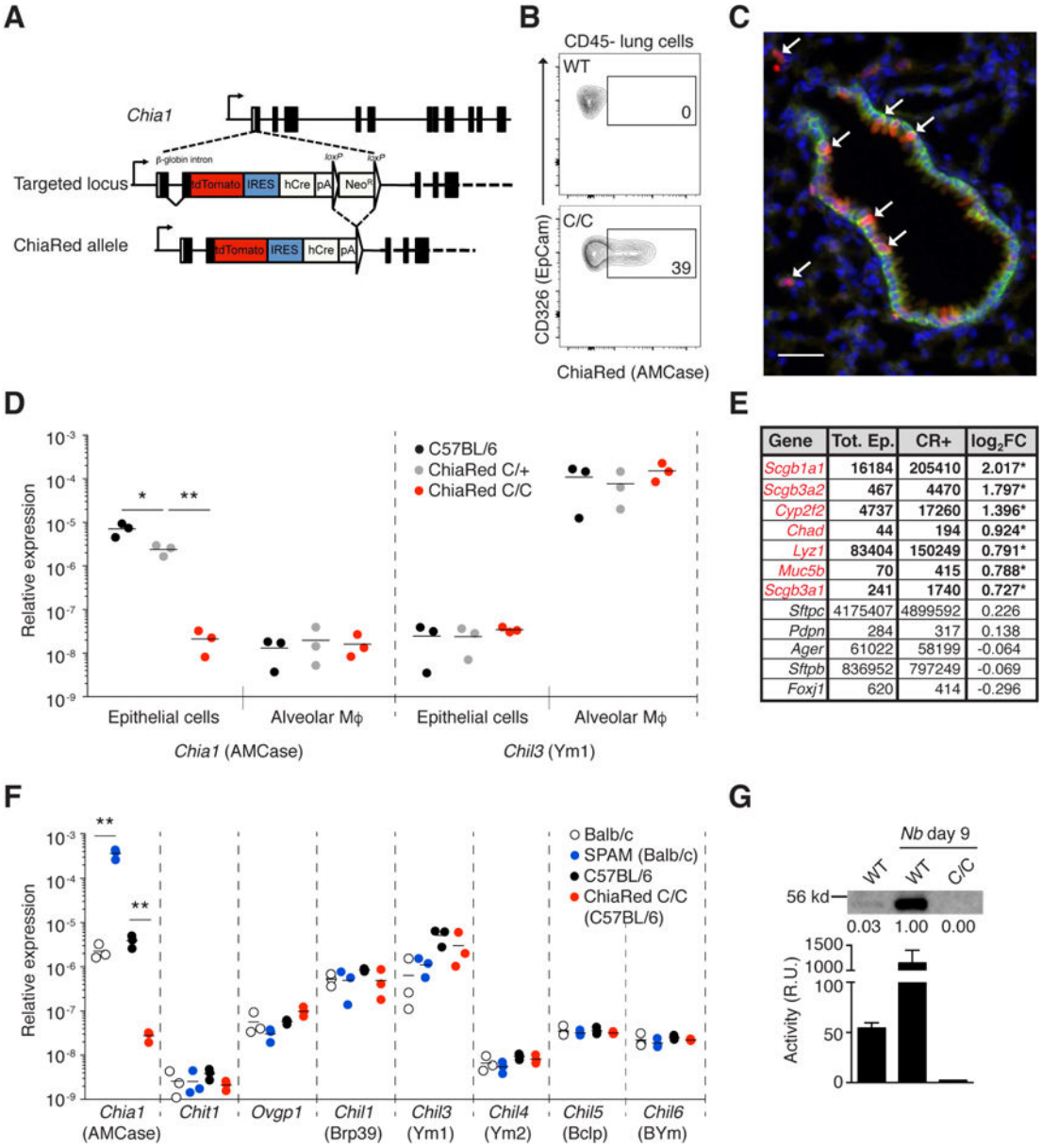

Gene	Tot. Ep.	CR+	log$_2$FC
Scgb1a1	16184	205410	2.017*
Scgb3a2	467	4470	1.797*
Cyp2f2	4737	17260	1.396*
Chad	44	194	0.924*
Lyz1	83404	150249	0.791*
Muc5b	70	415	0.788*
Scgb3a1	241	1740	0.727*
Sftpc	4175407	4899592	0.226
Pdpn	284	317	0.138
Ager	61022	58199	-0.064
Sftpb	836952	797249	-0.069
Foxj1	620	414	-0.296

FIGURE 1. Airway epithelial cells produce active AMCase

(**A**) AMCase (*Chia1*) gene targeting strategy and map of ChiaRed allele. (**B**) Flow cytometry for ChiaRed reporter expression among epithelial (CD45-EpCAM+) lung cells from wild-type (WT) and homozygous ChiaRed (C/C) mice. (**C**) Immunohistochemical localization of AMCase reporter-expressing cells (red, indicated by arrows; green, EpCAM; blue, DAPI) in lung tissue from WT and C/C mice; scale bar = 50 mm. (**D**) qPCR analysis of sorted epithelial cells (CD45-EpCAM+) and alveolar macrophages (CD45+CD11c+Siglec F+); genes normalized to *18s* expression and presented in relative units. (**E**) RNA-Seq analysis of select transcripts [fragments per kilobase of exon per million mapped reads (FPKM), averaged] among sorted ChiaRed+ (CR+) epithelial cells compared to total wild-type epithelial cells (Tot. Ep.). Significantly enriched genes (false discovery rate<0.05) denoted by red text and asterisks indicating log$_2$FC (fold change). (**F**) qPCR analysis of whole lung

RNA from indicated mice. (**G**) Western blot analysis of AMCase protein levels (top) and chitinase activity (bottom) in BAL fluid from indicated mice in the steady-state and 9 days after infection with *Nippostrongylus brasiliensis (Nb).* Numbers below blot indicate relative intensities by densitometry. R.U. = relative units. Data in (B, C, G) are representative of at least two independent experiments, and results from similar treatment groups were pooled in (G) and represent mean±SEM, n = 3/group. $^{*}p<0.01$ $^{**}p<0.001$ (unpaired t-test). See also Figure S1, Figure S2, and Table S1.

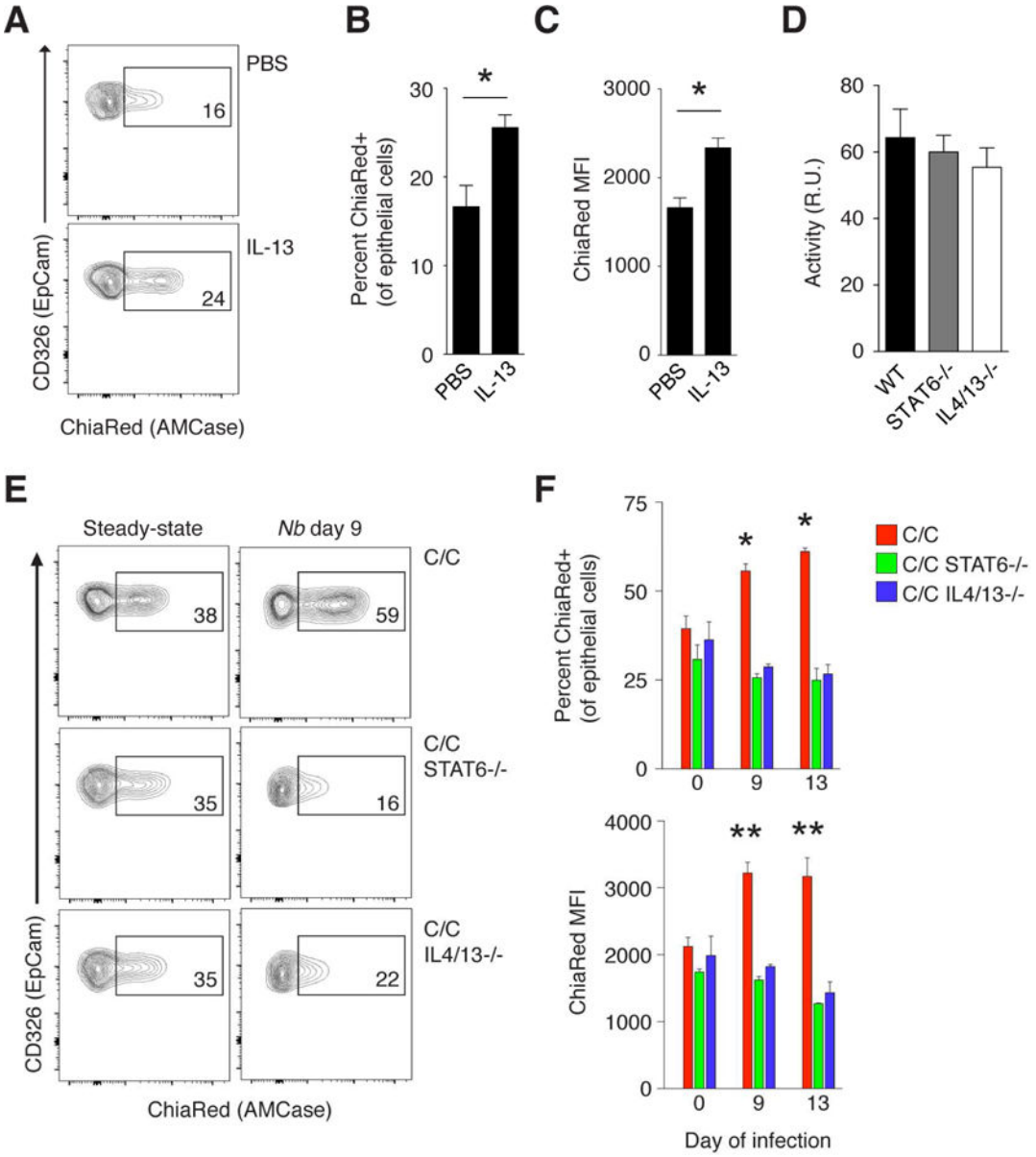

FIGURE 2. Constitutive AMCase expression is independent of type 2 cytokine signaling

(**A**) Flow cytometry of AMCase (ChiaRed) reporter expression, (**B**) percent ChiaRed+ epithelial cells, and (**C**) median fluorescence intensity (MFI) among lung epithelial cells (CD45-EpCAM+) from heterozygous ChiaRed (C/+) mice 48 hours after treatment with intranasal PBS or IL-13. (**D**) Chitinase activity in steady-state BAL fluid from indicated mice. (**E**) Flow cytometry of ChiaRed expression, (**F**) percent ChiaRed positive (top) and ChiaRed MFI (bottom) among lung epithelial cells from homozygous ChiaRed (C/C), C/C STAT6−/−, and C/C IL-4/IL-13−/−mice in the steady state or 9 days after *Nb* infection. Numbers in flow cytometry gates indicate percentage of ChiaRed+ cells among CD45-EpCAM+ lung cells. R.U. = relative units. Data are representative of at least two independent experiments, and results from similar treatment groups were pooled to represent

mean±SEM, n = 3–5 mice/group; $^{*}p<0.01$; $^{**}p<0.001$ (unpaired t-test), in (F) as compared to similar uninfected group. See also Figure S2.

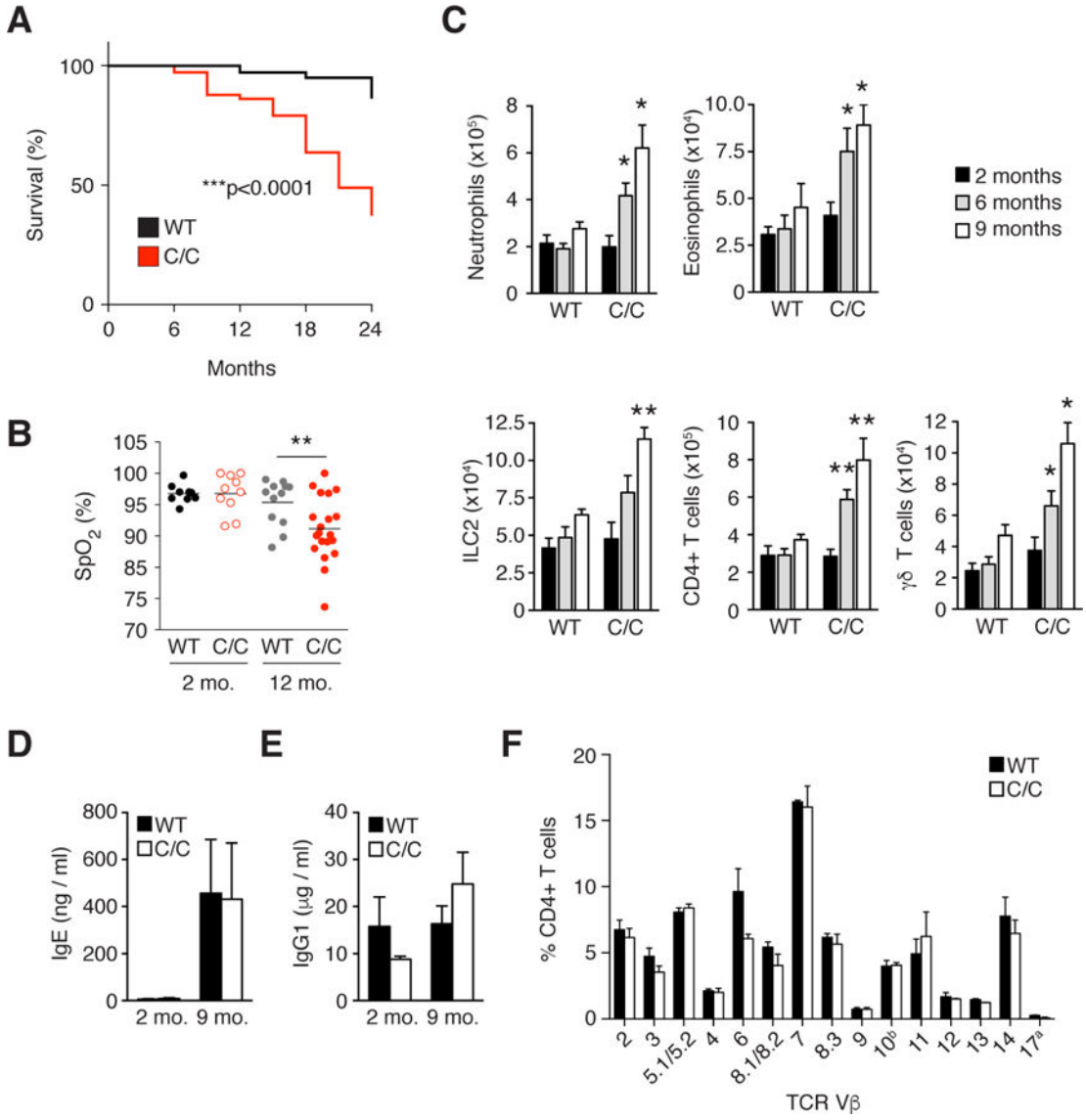

FIGURE 3. Constitutive AMCase maintains lifespan and lung health with aging

(**A**) Survival rates, (**B**) oxygen saturation levels (SpO_2), and (**C**) total lung cell inflammatory subsets among wild-type (WT) and homozygous ChiaRed (C/C) mice of indicated ages. Lung cell populations calculated as described in Figure S1C. (**D**) Total IgE and (**E**) IgG_1 antibody levels in the serum of WT and C/C mice of indicated ages. (**F**) Percent of lung CD4+ T cells from 9-month-old mice positive for indicated TCR Vp chains, analyzed by flow cytometry. Comparison of survival rates in (A) calculated by log-rank (Mantel-Cox) test; WT, n=44; C/C, n=36. Data in (C-F) are expressed as mean±SEM, n = 9–20/group in (B), 6–10/group in (C-E), and n = 3/group in (F). $^{*}p<0.01$; $^{**}p<0.001$ (unpaired t-test), in (B, C) as compared to similarly aged control group. See also Figures S3 and S4.

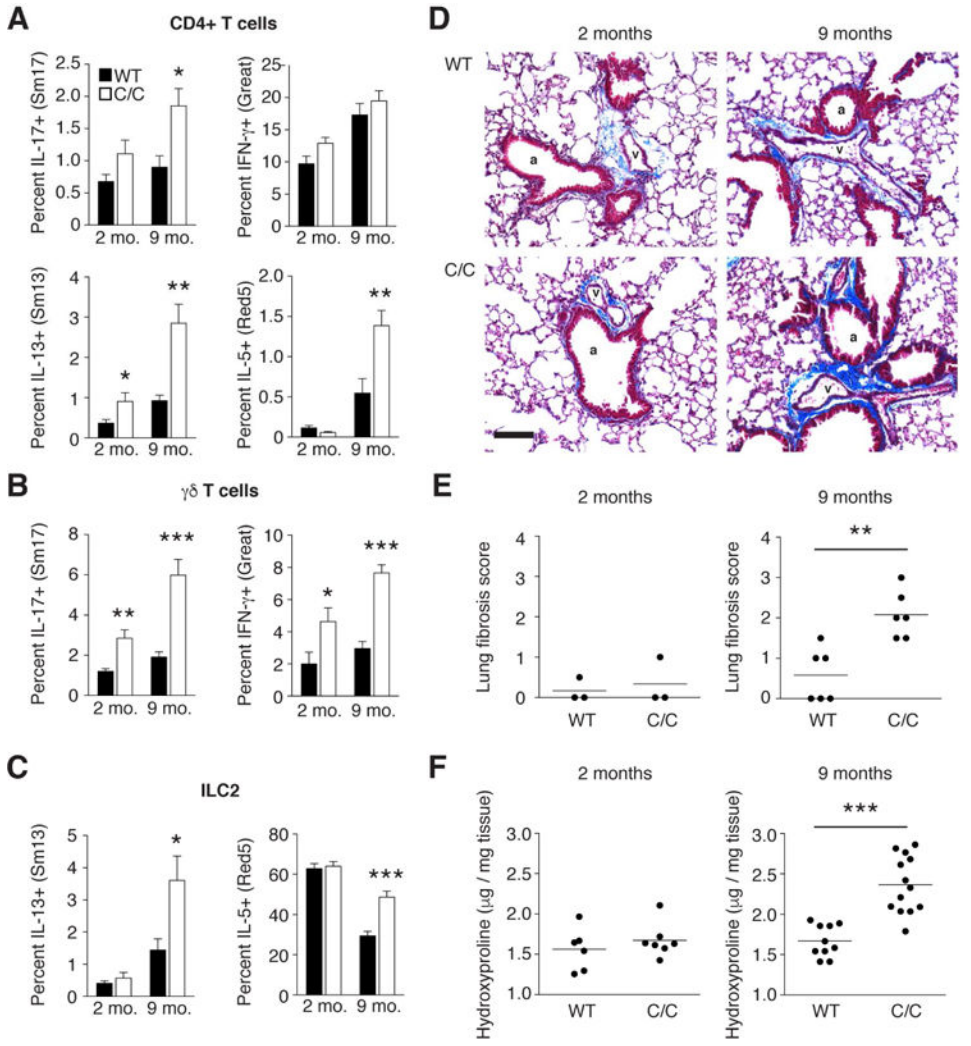

FIGURE 4. AMCase-deficient mice develop spontaneous age-related lung fibrosis

Expression of IL-17A (Sm17), IFNg (Great), IL-13 (Sm13), and IL-5 (Red5) cytokine reporters among (**A**) CD4+ T cells, (**B**) γδ T cells, and (**C**) ILC2s, analyzed ex vivo from lungs of WT and AMCase-deficient (C/C) mice of indicated ages. (**D**) Masson's trichrome-stained lung sections from 2-and 9-month old WT and C/C mice; scale bar = 100 pm, a = airway, v = vessel. (**E**) Lung fibrosis score and (**F**) hydroxyproline in lungs of WT and C/C mice. Data are representative of at least two independent experiments, and results from similar treatment groups were pooled to represent mean±SEM, n = 6–13 mice/group; $^{*}p<0.01$; $^{**}p<0.001$; $^{***}p<0.0001$ (unpaired t-test), as compared to age-matched WT control. See also Figures S3 and S4.

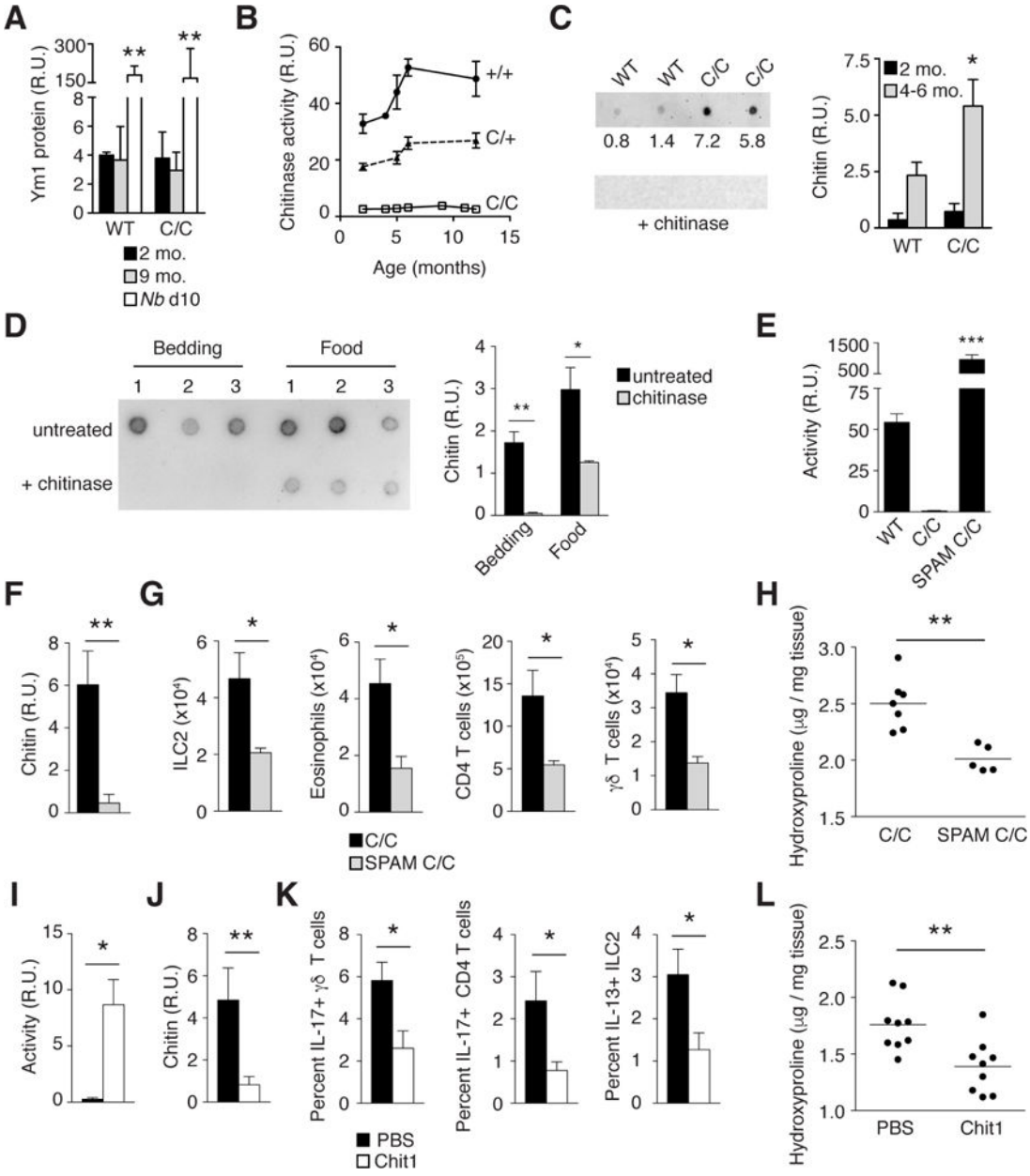

FIGURE 5. Chitin accumulates spontaneously in the airways of aged AMCase-deficient mice and contributes to fibrosis

(**A**) Ym1 protein levels in BAL fluid from WT and C/C mice, unchallenged and 10 days after *Nb* infection. (**B**) Chitinase activity in BAL fluid collected from unchallenged WT, C/+, and C/C mice at indicated ages. (**C**) Chitin-binding domain (CBD) blot of BAL fluid from the lungs of 4 month-old WT and C/C mice, before (top) and after (bottom) chitinase treatment. Numbers below blot indicate relative intensity of each dot analyzed by densitometry; summarized at right. (**D**) Representative CBD blot of extracts (1 μg dry weight) prepared from homogenized food and bedding collected from mouse cages housed in standard barrier conditions, before (top) and after (bottom) chitinase treatment. (**E**) Chitinase activity in BAL fluid collected from indicated mice. (**F**) Chitin amounts in BAL

fluid, measured by CBD, (**G**) lung tissue ILC2s, eosinophils, CD4+ T cells, γδ T cells, and (**H**) lung hydroxyproline content of indicated 9-month-old mice. (**I**) Chitinase activity and (**J**) chitin amounts in BAL fluid, (**K**) expression of IL-17A (Sm17) among γδ and CD4+ T cells and IL-13 (Sm13) among ILC2s, and (**L**) hydroxyproline content in lungs of aged C/C mice treated with PBS or Chit1. Data are representative of at least two independent experiments, and results from similar treatment groups were pooled to represent mean ±SEM, n = 3–10/group; *p<0.05; **p<0.01 (unpaired t-test), compared as indicated, or in (C), to age-matched WT control. R.U. = relative units. See also Figure S5.

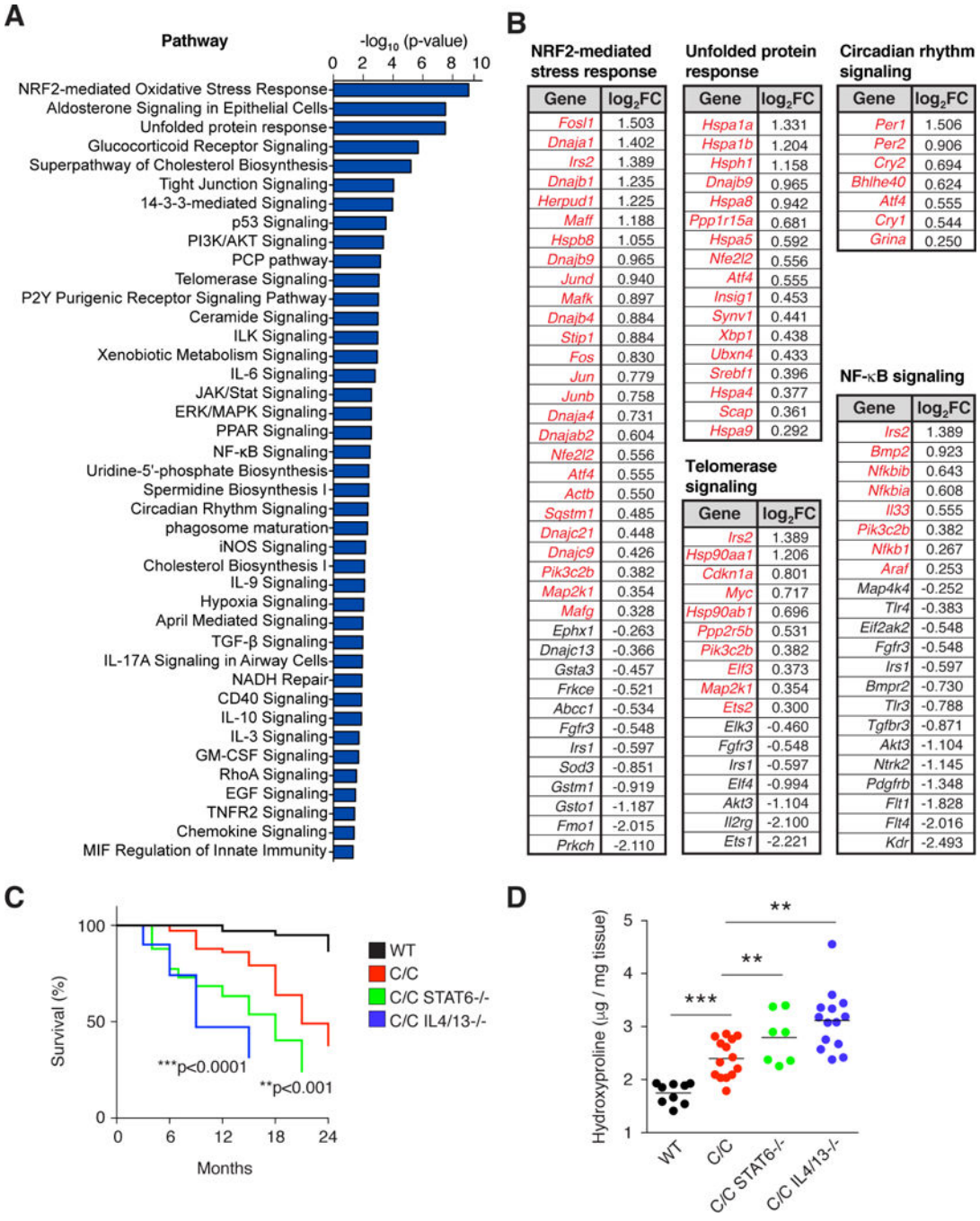

FIGURE 6. Cytokine signaling and cellular stress pathways induced in AMCase-deficient epithelium

(**A**) Analysis of selected differentially enriched canonical pathways and (**B**) selected gene sets enriched in C/C ChiaRed+ epithelial cells (ChiaRed+EpCAM+CD45-) as compared to cells isolated from C/+ mice. Significant enrichment identified by differential expression as $\log_2$FC (fold change); red, upregulated, black, downregulated. (**C**) Survival rates among indicated mice and (**D**) hydroxyproline content in lungs of indicated 12-month-old mice. Comparison of survival rates in (C) calculated by log-rank (MantelCox) test and p-values

indicate comparison to C/C; WT, n=44; C/C, n=36. C/C STAT6−/−, n=25; C/C IL4/13−/−, n=30. Lines in (D) represent mean value; $^{**}p<0.01$; $^{***}p<0.001$ (unpaired t-test). See also Figure S6, Table S2, and Table S3.

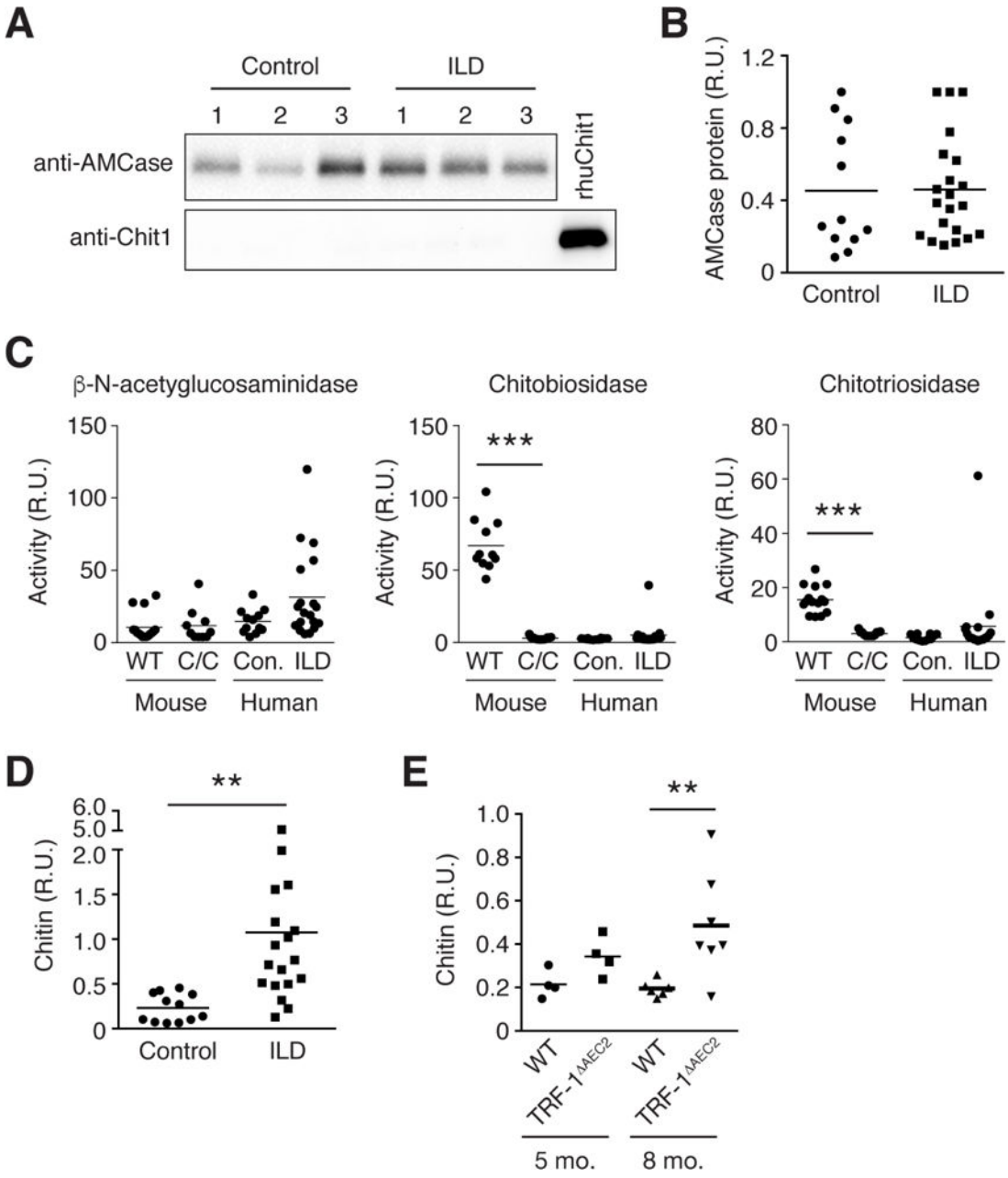

FIGURE 7. Human ILD patients accumulate chitin polymers in BAL fluid

(**A**) Representative Western blot analysis of AMCase and chitotriosidase (Chitl) proteins in human BAL fluid collected from healthy donors and ILD patients. Each lane represents distinct individual BAL fluid sample or recombinant human Chitl (rhuChitl). (**B**) Relative intensity values for AMCase protein expression by Western blot calculated by densitometry; individual experimental subjects plotted as single dots; control, n = 12; ILD, n = 21. (**C**) Chitinase activity in BAL fluid collected from mice of indicated genotype, healthy human controls (Con.), and ILD patients (ILD). (**D**) Chitin content, as measured by CBD blot, in BAL fluid collected from the lungs of healthy donors and ILD patients; individuals plotted as single dots; control, n = 12; ILD, n = 18. **(E**) Chitin content in BAL fluid from control

mice (WT) and those with conditional deletion of TRF-1 in type II alveolar epithelial cells (TRF-$1^{\Delta AEC2}$); individuals plotted as single dots; n = 4–7/group. R.U. = relative units. Lines in (B–D) represent mean value; $^{**}p<0.01$; $^{***}p<0.001$ (unpaired t-test), compared to healthy or similarly treated age-matched control. See also Figure S7 and Table S4.